UNCLASSIFIED

SECURITY CLASSIFICATION OF THIS PAGE (When Data Entered)

1

REPORT DOCUMENTATION PAGE

READ INSTRUCTIONS BEFORE COMPLETING FORM

1. REPORT NUMBER: AFIT/CI/NR 88- 34
2. GOVT ACCESSION NO.:
3. RECIPIENT'S CATALOG NUMBER:
4. TITLE (and Subtitle): ESTIMATING EVAPOTRANSPIRATION OF AN IRRIGATED SURFACE FROM UPWIND AND DOWNWIND VERTICAL PROFILES OF TEMPERATURE AND HUMIDITY
5. TYPE OF REPORT & PERIOD COVERED: MS THESIS
6. PERFORMING ORG. REPORT NUMBER:
7. AUTHOR(s): DAVID F. ZEHR
8. CONTRACT OR GRANT NUMBER(s):
9. PERFORMING ORGANIZATION NAME AND ADDRESS: AFIT STUDENT AT: UTAH STATE UNIVERSITY
10. PROGRAM ELEMENT, PROJECT, TASK AREA & WORK UNIT NUMBERS:
11. CONTROLLING OFFICE NAME AND ADDRESS:
12. REPORT DATE: 1988
13. NUMBER OF PAGES: 77
14. MONITORING AGENCY NAME & ADDRESS (if different from Controlling Office): AFIT/NR, Wright-Patterson AFB OH 45433-6583
15. SECURITY CLASS. (of this report): UNCLASSIFIED
15a. DECLASSIFICATION/DOWNGRADING SCHEDULE:
16. DISTRIBUTION STATEMENT (of this Report): DISTRIBUTED UNLIMITED: APPROVED FOR PUBLIC RELEASE

17. DISTRIBUTION STATEMENT (of the abstract entered in Block 20, if different from Report): SAME AS REPORT
18. SUPPLEMENTARY NOTES: Approved for Public Release: IAW AFR 190-1
LYNN E. WOLAVER 18 Jul 88
Dean for Research and Professional Development
Air Force Institute of Technology
Wright-Patterson AFB OH 45433-6583
19. KEY WORDS (Continue on reverse side if necessary and identify by block number):
20. ABSTRACT (Continue on reverse side if necessary and identify by block number): ATTACHED

DD FORM 1 JAN 73 1473 EDITION OF 1 NOV 65 IS OBSOLETE

UNCLASSIFIED

SECURITY CLASSIFICATION OF THIS PAGE (When Data Entered)

ABSTRACT

Estimating Evapotranspiration of an Irrigated Surface

From Upwind and Downwind Vertical Profiles of

Temperature and Humidity

by

David F. Zehr, Captian, USAF

Master of Science

Utah State University, 1988

Major Professor: Dr. Lawrence E. Hipps
Department: Soil Science and Biometeorology

The evapotranspiration (ET) and the contribution of the horizontal advection of sensible heat were predicted for an irrigated surface in arid regions from upwind and downwind vertical profiles of temperature and humidity. Measurements were made of temperature and specific humidity to a height of 70 meters at the upwind and downwind sides of an irrigated alfalfa field with dry upwind conditions.

The depth of air whose temperature and humidity profiles were distorted by the irrigated surface defined a control volume. Total ET was estimated from a vapor budget method, which essentially calculated the input of water vapor into the control volume. The amount of energy used in ET which was contributed by sensible heat advection was estimated by calculating the amount of internal energy depleted from the control volume. Simultaneous estimates of ET were made with an eddy correlation system, located

near the center of the field.

The depth of air modified by the irrigated crop averaged 10 meters for specific humidity and 15 meters for temperature during the light winds encountered in this study. ET estimates from the vapor budget method compared very well with the eddy correlation results. The deviation between the two estimates averaged 43 W m^{-2}, which translated into 7.2 percent.

Calculations of the depletion of internal energy in the control volume indicated that, in this study, the horizontal advection of sensible heat contributed from 35 to 86 percent of the total energy used in ET. These values further evidence the great importance of sensible heat advection in the water balance of arid regions.

These methods, though they are quite simple, appeared to work well in this study. However, it is necessary to measure the vertical profiles to an adequate height, which is greater than that usually considered by similar studies.

(77 pages)

ESTIMATING EVAPOTRANSPIRATION OF AN IRRIGATED SURFACE FROM UPWIND AND DOWNWIND VERTICAL PROFILES OF TEMPERATURE AND HUMIDITY

by

David F. Zehr, Captain, USAF

A thesis submitted in partial fulfillment
of the requirements for the degree
of
MASTER OF SCIENCE
in
Soil Science and Biometeorology

Approved:

Major Professor

Committee Member

Committee Member

Dean of Graduate Studies

UTAH STATE UNIVERSITY
Logan, Utah
1988

ACKNOWLEDGMENTS

The data acquisition, analysis and research was conducted under the supervision of Dr. Larry Hipps of the Department of Soil Science and Biometeorology at Utah State University.

I would like to thank Dr. Hipps for his patience, excellent guidance, support, and expertise, without which this project would not have been completed satisfactorily. Deepest appreciation to Dr. Hanks and Dr. Allen of my graduate committee who added a practical side to the research. A sincere thank you to Dr. Gail Bingham for stepping in at the end. Special thanks to Ray Jackson, Bruce Kimball, and the of the staff of the U.S. Water Conservation Laboratory, Phoenix, Arizona, who made available the opportunity to collect, share, and analyze data with them for the purpose of better understanding the boundary layer environment. A heartfelt thank you to Bill Munley, Eric Baiden, and Tan Hongbao for spending one week during June in 110 plus degree temperatures in Arizona collecting the data for this project.

I would like to thank Mike, for enduring E&M and patiently explaining Fortran programming to me, and the rest of my friends in the Biometeorology Department at Utah State. Finally thank you Belinda, Brandis, and Danielle.

David F. Zehr

ACADRERE TOTALITER

TABLE OF CONTENTS

LIST OF TABLES

LIST OF TABLES (Continued)

LIST OF TABLES (Continued)

LIST OF FIGURES

LIST OF FIGURES (Continued)

LIST OF TERMS AND SYMBOLS

Symbol

ET' - evapotranspiration due solely to the affect of horizontal advection of sensible heat ($W\ m^{-2}$).

$\overline{U}$ - mean wind speed ($m\ sec^{-1}$).

Z - altitude or height (m).

X - downwind direction or fetch (m).

ZAGL- height above ground level (m).

Z_i - height of the temperature inversion layer (m).

Z_w - height of the enhanced water vapor layer (m).

θ - potential temperature (°K).

q - specific humidity ($Kg_w\ Kg_a^{-1}$).

BREB- Bowen-Ratio Energy Budget.

$\overline{ET}$ - average evapotranspiration rate as measured by the vapor budget method ($W\ m^{-2}$).

W - rate at which water vapor transits the control volume ($W\ m^{-2}$).

LE - latent heat flux density.

L - latent heat of vaporization ($2.45 \times 10^6\ J\ Kg^{-1}$).

ρ_a - density of moist air ($Kg_w\ m^{-3}$).

C_p - specific heat of moist air at constant pressure (1004 $J\ Kg_a^{-1}\ °K^{-1}$).

H - sensible heat (°K).

ET - total evapotranspiration rate ($W\ m^{-2}$).

Rn - net radiation ($W\ m^{-2}$).

S - soil heat flux density.

w' - instantaneous departure from the mean of vertical wind speed ($m\ sec^{-1}$).

LIST OF TERMS AND SYMBOLS (Continued)

Symbol

q' - instantaneous departure from the mean of specific humidity ($Kg_w\ sec^{-1}$).

T_v - virtual temperature (°K).

e_s - saturated vapor pressure (mb).

e_a - actual vapor pressure (mb).

e_w - saturated vapor pressure over a plane surface of pure ordinary liquid (mb).

T - absolute temperature (°K).

T_s - steam point temperature (373.16 °K).

e_{ws} - saturated vapor pressure of pure ordinary liquid water at steam point temperature (1 standard atmosphere = 1013.246 mb).

p - pressure in (mb).

ϵ - ratio of the mass of water to the mass of air (.622).

T_w - wet bulb temperature (°K).

R_d - gas constant for dry air ($287\ J\ °K^{-1}\ Kg^{-1}$).

K_h - exchange coefficient for sensible heat.

K_w - exchange coefficient for water vapor.

ABSTRACT

Estimating Evapotranspiration of an Irrigated Surface From Upwind and Downwind Vertical Profiles of Temperature and Humidity

by

David F. Zehr, Master of Science

Utah State University, 1988

Major Professor: Dr. Lawrence E. Hipps
Department: Soil Science and Biometeorology

The evapotranspiration (ET) and the contribution of the horizontal advection of sensible heat were predicted for an irrigated surface in arid regions from upwind and downwind vertical profiles of temperature and humidity. Measurements were made of temperature and specific humidity to a height of 70 meters at the upwind and downwind sides of an irrigated alfalfa field with dry upwind conditions.

The depth of air whose temperature and humidity profiles were distorted by the irrigated surface defined a control volume. Total ET was estimated from a vapor budget method, which essentially calculated the input of water vapor into the control volume. The amount of energy used in ET which was contributed by sensible heat advection was estimated by calculating the amount of internal energy depleted from the control volume. Simultaneous estimates of ET were made with an eddy correlation system, located

near the center of the field.

The depth of air modified by the irrigated crop averaged 10 meters for specific humidity and 15 meters for temperature during the light winds encountered in this study. ET estimates from the vapor budget method compared very well with the eddy correlation results. The deviation between the two estimates averaged 43 W m^{-2}, which translated into 7.2 percent.

Calculations of the depletion of internal energy in the control volume indicated that in this study, the horizontal advection of sensible heat contributed from 35 to 86 percent of the total energy used in ET. These values further evidence the great importance of sensible heat advection in the water balance of arid regions.

These methods, though they are quite simple, appeared to work well in this study. However, it is necessary to measure the vertical profiles to an adequate height, which is greater than that usually considered by similar studies.

(77 pages)

INTRODUCTION

Due to the critical importance of water in the biosphere, micrometeorologists have become concerned about the role of water loss due to evapotranspiration into the atmosphere, especially in semi-arid and arid regions of the world. In these arid regions it is not uncommon for annual evapotranspiration rates to far exceed annual precipitation rates when irrigation is applied (Inmula and Sill, 1985).

Therefore, one of the important applications of micrometeorology is to evaluate the processes controlling the energy and water balances of agricultural lands. Many micrometeorological studies of these problems have assumed or tried to ensure horizontal homogeneity at and/or near the surface. In other words the advection of sensible heat has been ignored or assumed to be non-existent. Horizontal homogeneity seldom occurs in nature. A well-irrigated field (an oasis) surrounded by dry land is clearly not a homogeneous surface. Recent studies have indicated that the advection of sensible heat can be a significant contribution to the energy and water balance in arid regions (Abdel-Aziz et al., 1964; Rosenberg, 1969; Brakke et al., 1978). Rosenberg and Verma (1978) have reported that evapotranspiration by irrigated crops in semi-arid regions can exceed net radiation by a factor of two or more due to the additional energy supplied by advection.

Advection is defined by the Glossary of Meteorology (Huschke, 1959, p. 10) as "the process of transport of an atmospheric property solely by the mass motion of the atmosphere...". When the mean wind blows along a temperature gradient, for example from hotter, dry upwind fields to cooler, wetter downwind fields, advection of sensible heat occurs. This advective condition is referred to as local advection (Hanks et al., 1971; Brakke et al., 1978). Regional advection occurs when the horizontal transport of sensible heat is due to the movement of warm, dry air masses on the synoptic scale (Blad and Rosenberg, 1974). More often than not, both scales of advection will occur simultaneously.

The advected sensible heat from dry upwind conditions will increase the amount of energy available for evapotranspiration and the vapor pressure gradient between the advected parcel of air and the crop canopy. As this parcel of air moves downwind over the crop canopy it cools, resulting in a temperature and humidity difference between the leading edge and the downwind edge of the crop canopy (Oke, 1978).

Attempts to understand how advection influences the microclimate have resulted in numerous studies of the changes of the microclimate downwind of a leading edge of a surface discontinuity. Results of several studies have suggested that advection of sensible heat may be a critical part of the energy and water balance of agricultural lands,

and that the assumption of horizontal homogeneity may distort results of some experiments. In order to better understand the advective process, several studies have modeled the changes in temperature and humidity profiles downwind of a leading edge for a given rate of evapotranspiration. It is important to note that these studies of advection have been restricted to very shallow layers of the atmosphere that were usually only a few meters deep.

Objectives

The objective of this study is to calculate short term rates of evapotranspiration and the advective contribution towards these evapotranspiration rates from measurements of the downwind distortion of temperature and humidity profiles over an irrigated crop. The specific objectives follow.

1. Vapor Budget Method

Using a modified vapor budget method, estimate evapotranspiration rates using the assumption of conservation of mass. The amount of specific humidity input to a control volume from the surface will be calculated by measuring the amount of water vapor coming in and going out of the control volume. The control volume will be defined by the surface area of the evapotranspiring crop to the height of the enhanced water vapor layer. These estimates of the evapotranspiration rates will be

compared with evapotranspiration rates measured by an eddy correlation system located just above the top of the crop canopy.

2. Internal Energy Method

Calculate the depletion of internal energy in the air volume as it passes over the irrigated crop from the change in the vertical profiles of temperature between upwind and downwind locations. From the First Law of Thermodynamics, this change in internal energy represents the total contribution towards evapotranspiration from the horizontal advection of sensible heat.

LITERATURE REVIEW

When a parcel of air passes over a surface discontinuity, a boundary layer gradually develops as shown in Fig. 1. The layer of the atmosphere whose characteristics such as temperature and humidity have been modified by the new surface is commonly called the internal boundary layer. The depth of this internal boundary layer increases downwind of the surface discontinuity and commonly requires a fetch of between 10 to 30 meters for every meter increase in height. The rate at which the internal boundary layer develops is dependent on the relative change of roughness between the two dissimilar surfaces and the state of atmospheric stability (Oke, 1978). Within the internal boundary layer exists a layer of air that is fully adjusted to the characteristics of the new surface that it has passed over, and a new equilibrium is established within it. The fully adjusted layer is about 10 percent of the depth of the total internal boundary layer.

In the upper portion of the internal boundary layer, the transition zone, characteristics of the air parcel are still adjusting to the new surface conditions. Above the internal boundary layer the air is still influenced by upwind conditions, whether local or regional. During horizontal sensible heat advection, sensible heat is removed and moisture is input into the internal boundary

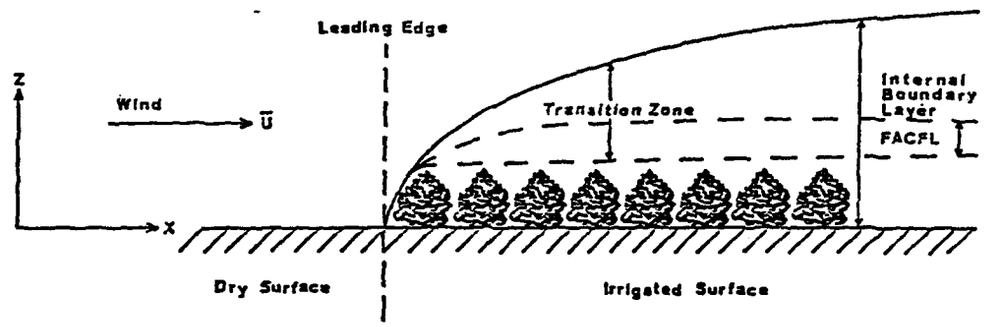

Fig. 1. The development of an internal boundary layer downwind of a leading edge under conditions of sensible heat advection. FACL is the fully adjusted constant flux layer.

layer by evapotranspiration and subsequently carried downwind. FACFL is the fully adjusted constant flux layer. Figs. 2a and 2b depict the anticipated adjustment of the potential temperature and specific humidity profiles as an air parcel travels from a hot, dry surface over a cooler, wet surface. The surface discontinuity is usually referred to as the leading edge.

The problems of leading edge effects on microclimates have been the topic of both theoretical and experimental studies. Philip (1959) published a paper on the theory of local advection in which he presented methods for solving the two-dimensional atmospheric-diffusion equation related to concentration, flux, and radiation types of boundary conditions.

A numerical model of airflow above changes in surface heat flux, temperature, and roughness for neutral and unstable conditions was developed by Taylor (1970). This model was based on boundary layer approximations, the Businger-Dyer hypothesis for the non-dimensional wind shear and heat flux, and a mixing-length hypothesis. No comparison of results with any other theories were given until he extended this model to include the stable case (Taylor, 1971). Taylor stated that "tolerable agreement" was achieved when comparisons were made with experimental results given by Rider et al. (1963). In theory, the error introduced by local advection toward the calculation of evapotranspiration using Bowen Ratio techniques (Hanks et

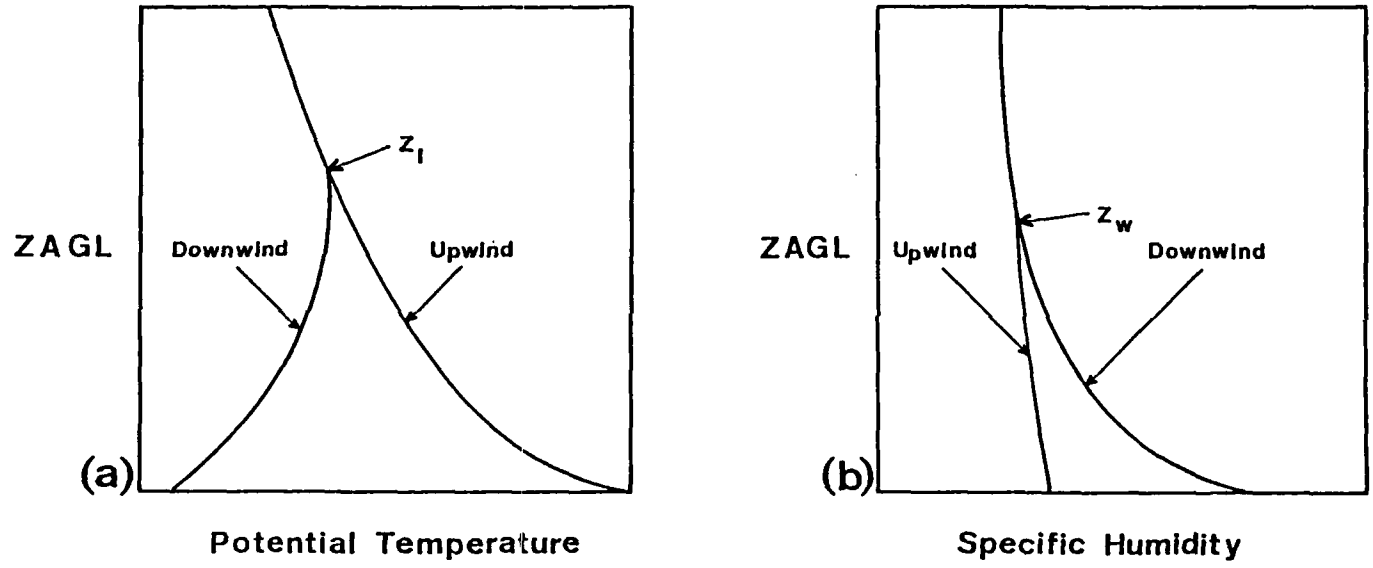

Fig. 2. Anticipated adjustments of vertical profiles of (a) potential temperature (θ) and (b) specific humidity (q) downwind of a leading edge.

al. 1971) may be minimized by additional measurements. Lang (1973) showed theoretically that the errors induced by calculating evapotranspiration in terms of the Bowen ratio can be avoided by additional measurements of wind speeds and horizontal gradients of humidity and temperature over a range of heights. A simple first-order correction for the error was suggested using measurements of horizontal gradients at a single height. However, many additional measurements are required.

The effect of an abrupt change of roughness at a leading edge on the mean flow and turbulent structure within an internal boundary layer was investigated by Rao et al. (1974a, 1974b), using a higher-order closure model. The model included dynamical equations for Reynolds stresses and the viscous dissipation rate. Their model predicted the distribution of mean wind, shear stress, turbulent energy, and other quantities with no "a priori" assumptions regarding any upwind values of these variables. They calculated that the internal boundary layer grew according to a 4/5ths power law, and that the height-to-fetch ratio of the fully adjusted layer was approximately 1/100 for a smooth-to-rough transition. They also reported that only the lower 10 percent of the internal boundary layer was fully adjusted to the new surface conditions. They compared their predicted profiles of temperature and humidity with the observed ones of Rider et al. (1963) and reported good agreement.

A study conducted by Blad and Rosenberg (1974) on a lysimetric evaluation of the Bowen-Ratio Energy Balance (BREB) method for evapotranspiration in the central Great Plains showed good agreement between the BREB method and lysimetric measurements of evapotranspiration under non-advective conditions. During advective conditions, however, the BREB method underestimated evapotranspiration by approximately 20 percent. They suggested that the 20 percent difference was primarily due to the assumption of equality of the exchange coefficients for heat and water vapor, which is an integral part of the BREB method. Verma et al. (1978) found that the exchange coefficients for sensible heat (K_h) were generally greater than the exchange coefficient for water (K_w) under advective conditions. This result contradicts the usual assumption of equality between K_h and K_w.

Numerous other studies have looked at the measured changes of the microclimate downwind of the leading edge of a surface discontinuity. Rider et al. (1963), observed the variation of temperature and humidity with distance downwind of a leading edge over a 50 square meter grass surface to a depth of 1.5 meters. They noted a general increase in humidity and a general decrease in temperature, with the greatest changes in humidity and temperature occurring closest to the ground. Abdel-Aziz et al. (1964) tested the Penman formula and four modifications. It was found that the formula consistently underestimated

evapotranspiration. Neither the formula nor the modifications to it could accurately account for the advection of sensible heat in semi-arid conditions. Dyer and Crawford (1965) observed the changes in the microclimate of a heavily irrigated grass field within dry surroundings. The field measured 355 meters by 146 meters. Their temperature profiles showed that continuous modification of the microclimate existed up to the maximum height of measurement (5 meters), even at a distance 200 meters downwind of the leading edge. They suggested that, to assume horizontal homogeneity, a site of considerable extent is required for micrometeorological and agricultural studies.

Hanks et al. (1971) suggested the importance of advection as a source of energy for evapotranspiration. They noted that temperature inversions occurred consistently over the crop during mid-afternoon due to the transfer of sensible heat by regional advection. Local advection was manifested by horizontal temperature and humidity gradients that were most evident from the leading edge to 40 meters downwind.

Brakke et al. (1978) measured temperature and humidity profiles within a 2-meter deep by 200-meter distance downwind over a well-irrigated crop canopy with relatively dry upwind conditions. Profiles were measured at several locations downwind of the leading edge. Under advective conditions their temperature profiles were inverted

downwind of the leading edge while the humidity profiles were lapse (decreasing with height). This showed a depletion of energy from the warm, dry, advected air directed towards the surface and an upward flux of water vapor within the internal boundary layer due to the evapotranspiring canopy. They calculated that between 15 and 50 percent of the total energy used in evapotranspiration on a daily basis came from sensible heat advection. The enhancement of evapotranspiration during advective conditions was shown by Baldocchi et al. (1981) to decrease water use efficiency. This results from the fact that the sensible heat energy supplied by advection can evaporate water but cannot contribute to photosynthesis.

Rosenberg and Verma (1978) examined the rate of evapotranspiration by an irrigated alfalfa crop during drought conditions. They found that on each day of the study the ratio of the latent heat flux density (LE) to the sum of the net radiation and soil heat flux (Rn + S) was such that $LE/(Rn + S) > 1$. This indicated that significant advection of sensible heat was occurring, providing the extra energy for the high evapotranspiration rates that were measured. It was observed by Motha et al. (1979) that temperature profiles were inverted over an irrigated crop canopy during advective conditions up to a height of 16 meters, the highest point of measurement. Their results indicated that turbulent mixing is effectively maintained

under advective conditions, resulting in the transport of large quantities of sensible heat to the crop and water vapor away from the crop. Turbulent intensities were found to be maintained at fairly high values during these times, even though the local temperature gradients suggested very stable conditions.

The previously cited studies of this "oasis" phenomenon have focused on the prediction of the distortion of downwind profiles of temperature and humidity, in which the evapotranspiration rate is an important controlling factor. However, the problem can be approached from an opposite point of view.

Can the rate of evapotranspiration and the effects of advection be estimated from measurements of the changes in temperature and humidity profiles?

Inmula and Sill (1985) proposed a technique for the short-term measurement of evaporation from well-irrigated crop canopies based on a control volume concept. Both upwind and downwind temperature and humidity profiles were measured over a tiny, 9.3-square meter simulated, crop surface to a height of 3 meters. Their downwind temperature profiles were inverted but not to as great an extent as other studies have noted. This was due to upwind conditions consisting of mown grass. Thus, there was not a large difference in upwind surface characteristics as opposed to the area under study. The rate of evaporation from the surface was calculated from the basic equation

$$ET = W \int_0^{Z_w} U \, (q_{downwind} - q_{upwind}) \, dz \qquad [1]$$

Where W is the width of their control volume, U the wind speed of a parcel of air that is entering the control volume, q the water vapor concentration of the air, and Z_w is the top of the enhanced vapor boundary layer on the downwind side. They visually fit a single temperature and wind profile to both the upwind and downwind temperature and wind data for use in calculating U and q.

For comparison evaporation was also calculated using a water budget method. This method involved the maintenance of a water budget for the control volume and can be stated as

$$E = S + I + P - O - G \qquad [2]$$

Here S is storage, I surface inflow, P precipitation, O surface outflow, and G subsurface seepage. This method is simple in theory but tedious in application. This is because the variables in equation [2] are difficult to measure. Also, in comparison to evaporation (E), some of the terms are quite large. Thus small errors in the measurement of one of these variables results in large errors in evaporation. Finally, the dynamic change of the stored water when subjected to large temperature extremes introduces another source of error. Inmula and Sill claim

that the water balance method is best applied for periods of 1 year or more.

They reported that comparison of the vapor budget values obtained from equation [1] compared well with those obtained from equation [2] under the following conditions:

1. Wind direction was constant enough that the downwind station was not required to be moved from one place to another during a profile measurement period of 15 minutes.
2. The number of average points at each height was at least four.
3. The wind speed at the 3 meter height was at least 2 m sec^{-1}.
4. Profiles contained no obviously spurious data points.

Deviations ranged from 1 to 30 percent with an average "error" of 12 percent.

Even though the previous studies cited examined the change of a microclimate downwind from a leading edge, they all only considered a shallow layer of the atmosphere. The above study was able to estimate evaporation from the downwind adjustment of only shallow profiles because the evaporating surface was very small (9.3 square meters). A typical irrigated field will modify the profiles to a much larger depth than any of the above-cited studies have examined.

Hipps et al. (1988) have demonstrated the depth at which the atmosphere is influenced by the transition from a

dry to an irrigated surface. That is, the depth at which the profiles of temperature and humidity are distorted. They sampled temperature and humidity profiles to a height of 70 meters using a tethered balloon system upwind and downwind of a well-irrigated alfalfa crop, 250 meters by 334 meters, surrounded by very dry conditions. Results showed the depth at which the profiles were distorted grew to as great as 30 meters after a 300-meter traverse over the irrigated surface. This suggests that large-scale eddies were dominating the transport of sensible heat down towards the crop and humidity upwards away from the crop. Clearly, a rather deep layer of air supplies sensible heat to the evaporating surface during advective conditions. Therefore, in order to properly examine the actual downwind change in profiles of temperature and humidity, this rather deep layer of the lower atmosphere must be considered.

THEORETICAL CONSIDERATIONS

Advection

Advection is usually defined as the transfer of an atmospheric property solely due to the mass motions of the atmosphere. The horizontal advection of sensible heat occurs when the mean wind blows with a component along a horizontal temperature gradient. This is generally expressed mathematically as

$$\bar{V}_h \cdot \nabla_h T \qquad [3]$$

Where $\bar{V}_h$ is the horizontal wind vector, ∇_h is the horizontal gradient operator defined as $[\delta/\delta x\ \hat{i} + \delta/\delta y\ \hat{j}]$, and T is temperature.

Vapor Budget Method

The water-vapor budget method uses a control volume to account for water vapor as it flows into and out of the system under study. For this study a control volume was defined by the edges of the crop and topped by the height of the enhanced water vapor layer. This height is taken as the height at which the upwind and downwind vertical profiles of specific humidity converge (Fig. 2b). The conservation equation for water vapor over a well-irrigated transpiring surface for the control volume can be written as

$$\overline{ET} = W_{downwind} - W_{upwind} \qquad [4]$$

Where $\overline{ET}$ is the average evapotranspiration rate in W m^{-2} and W is the rate at which the water vapor of the air enters the control volume upwind or leaves the control volume downwind. This states that the amount of water vapor input to the control volume from the surface ($\overline{ET}$) is equal to the difference between the water vapor input to the control volume from upstream and the amount of water vapor exiting the control volume downstream (Fig. 3). This assumes that the net flux of water vapor out of the top of the control volume is zero. It is also assumed that no net sideways or lateral (Y direction) transport is occurring.

The amount of water vapor added to the control volume from the surface is essentially given by the area between the upwind and downwind humidity profiles. The evapotranspiration rate can be calculated from knowledge of the water vapor input into the control volume if the residence time of a parcel of air over the evapotranspiring surface is known. This is because at any given rate of evapotranspiration, the longer the air is above the field the greater the amount of water vapor it can receive from below. The residence time is determined from the mean velocity of the wind flow and the distanced traversed over the new surface. Thus, the evapotranspiration rate is given by

$$\overline{ET} = \frac{L}{X} \int_0^{z_w} \bar{U}\, \rho_a(z) \left[q_d(z) - q_u(z) \right] dz \qquad [5]$$

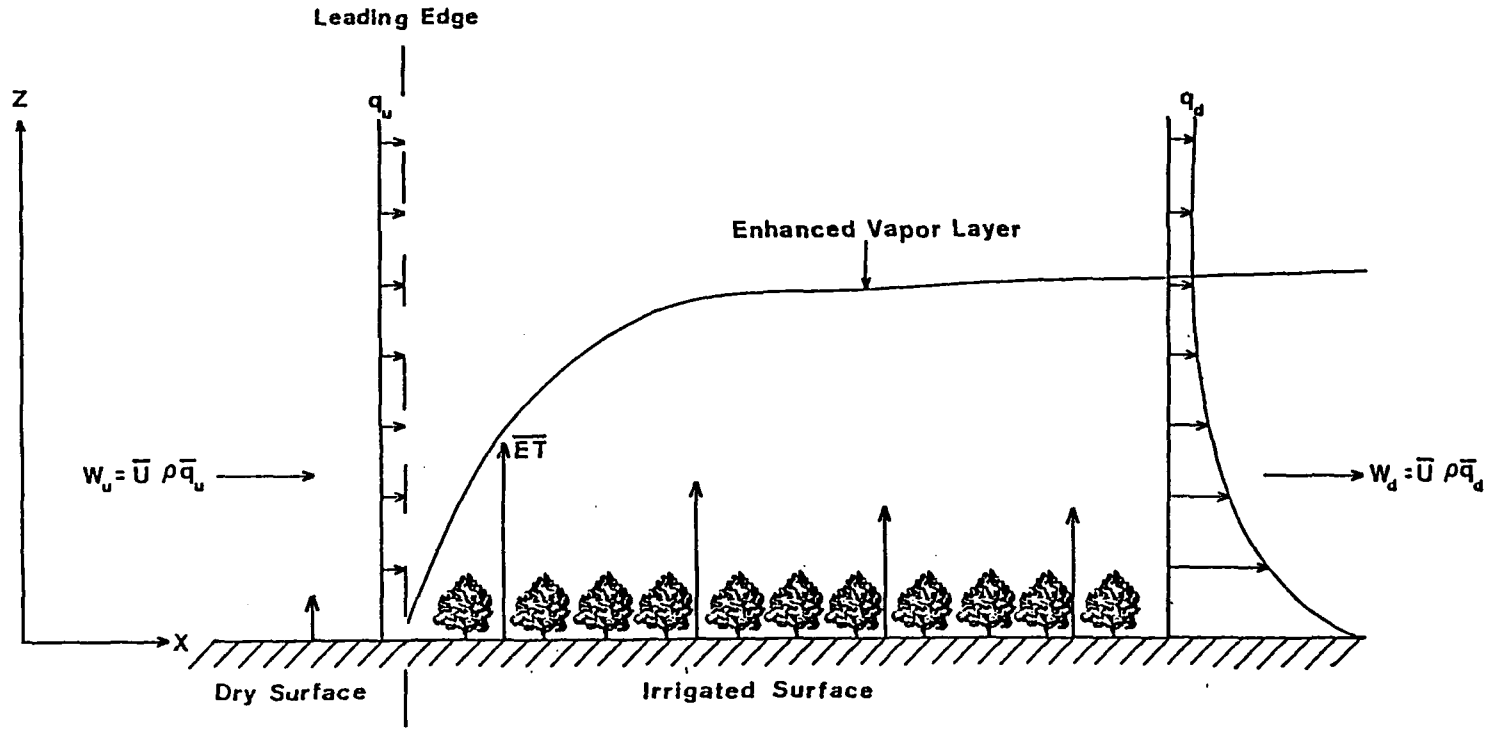

Fig. 3. Moisture advection from a hot, dry surface to a cooler, wetter surface. ET rates are proportional to arrow lengths.

Where ρ_a is the density of moist air (Kg m^{-3}) at any given height z, L is the latent heat of vaporization (J Kg^{-1}), q_d and q_u are the specific humidities at any given height z, downwind and upwind respectively, $\overline{U}$ is the mean wind speed of the parcel of air as it passes through the control volume, X the downwind length traversed by the control volume, and Z_w is the height of the enhanced water vapor layer.

Internal Energy Method

When sensible heat is advected over an irrigated surface, a vertical transport of heat towards the cooler surface occurs. Internal energy is removed from the parcel of air, thus reducing its temperature. The First Law of Thermodynamics implies in this case that the heat energy removed from the air parcel has been consumed in latent heat (LE). The amount of internal energy removed from the parcel of air by evapotranspiration is essentially equal to the area between the upwind and downwind vertical temperature profiles and topped by the height of the temperature inversion (Fig. 2a). When the residence time of the control volume is considered, the portion of the evapotranspiration rate due solely to the advection of sensible heat can be written as

$$ET' = \frac{C_p}{X} \int_0^{Z_i} \overline{U}\, \rho_a(z) \left[\theta_u(z) - \theta_d(z)\right] dz \qquad [6]$$

Where ET′ is in W m^{-2}, C_p is specific heat of moist air (1004 J Kg_{air}^{-1} $°K^{-1}$), θ_u and θ_d are potential temperatures at any given height z, upwind and downwind respectively, Z_i is the height of the developed temperature inversion, and ρ_a, $\overline{U}$, and X are the same as defined previously in equation [5]. This equation reveals the contribution towards evapotranspiration (ET′) solely from the horizontal advection of sensible heat.

MATERIALS AND METHODS

Experimental Site

This project deals with horizontal advection of sensible heat brought about by a surface discontinuity. Therefore, an oasis type of environment was sought. An oasis environment exists when an irrigated crop is surrounded by a drier upwind surface. In this type of environment the air above the upwind surface is hotter and has a lower vapor pressure (e_a) than air over the crop. This provides an extra source of energy for evapotranspiration (Hamlyn, 1983) resulting in cooler, and more moist air over the crop.

In coordination with the U.S. Water Conservation Laboratory in Phoenix, Arizona, the use of the University of Arizona Maricopa Agricultural Center (MAC) farm was obtained during a project sponsored by the U.S.D.A. from 10 to 14 June 1987. This farm is located approximately 75 kilometers south of Phoenix and 28 kilometers west of U.S. Interstate Highway 10 (Fig. 4). The experimental plot was a well-watered alfalfa crop which measured 172 meters by 500 meters (8.6×10^4 m^2) (Fig. 5).

Data Acquisition

To apply the water vapor and energy budget methods properly requires the evaluation of both upwind and downwind temperature and humidity profiles to the top of the developing internal boundary layer. When air is

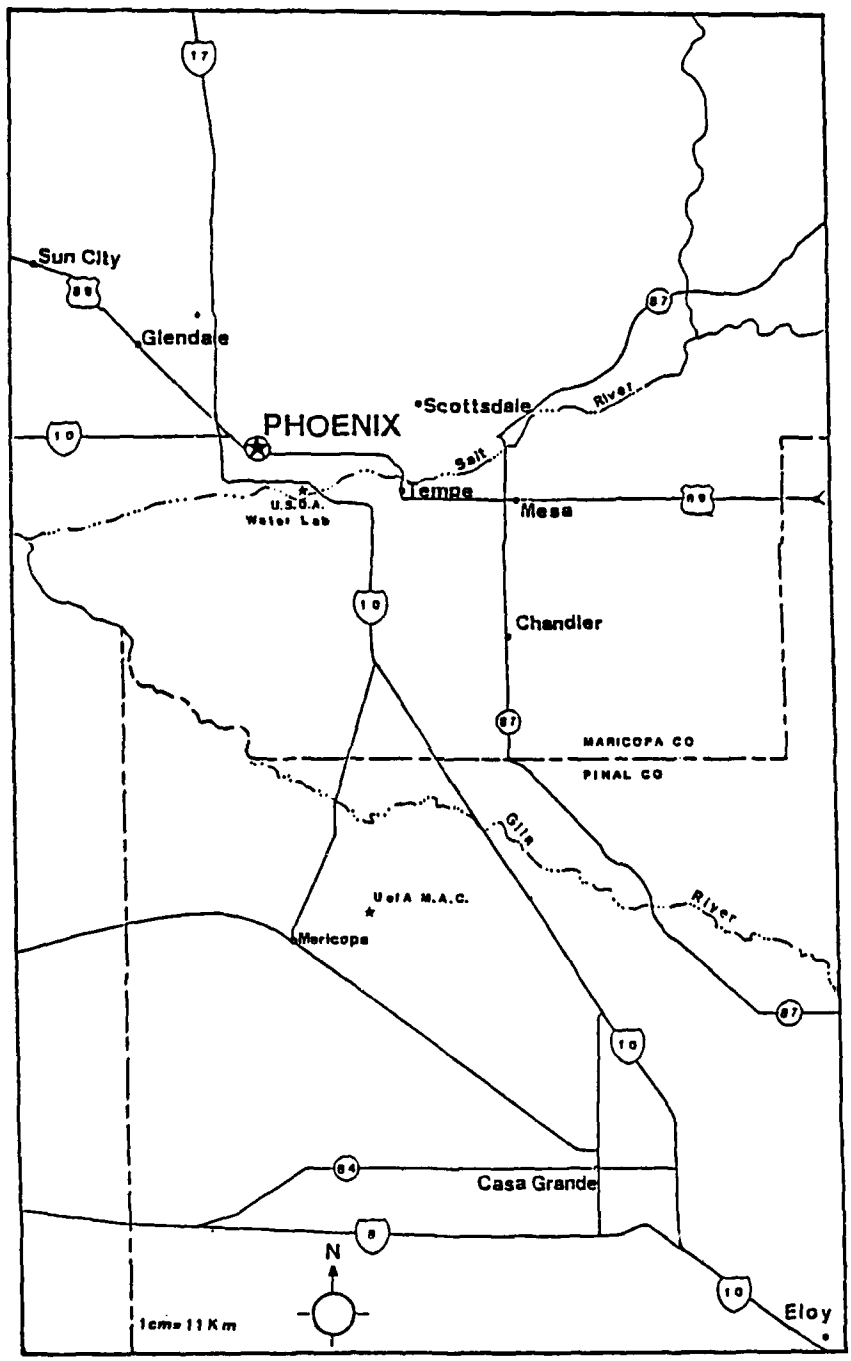

Fig. 4. Location of the University of Arizona Maricopa Agricultural Center.

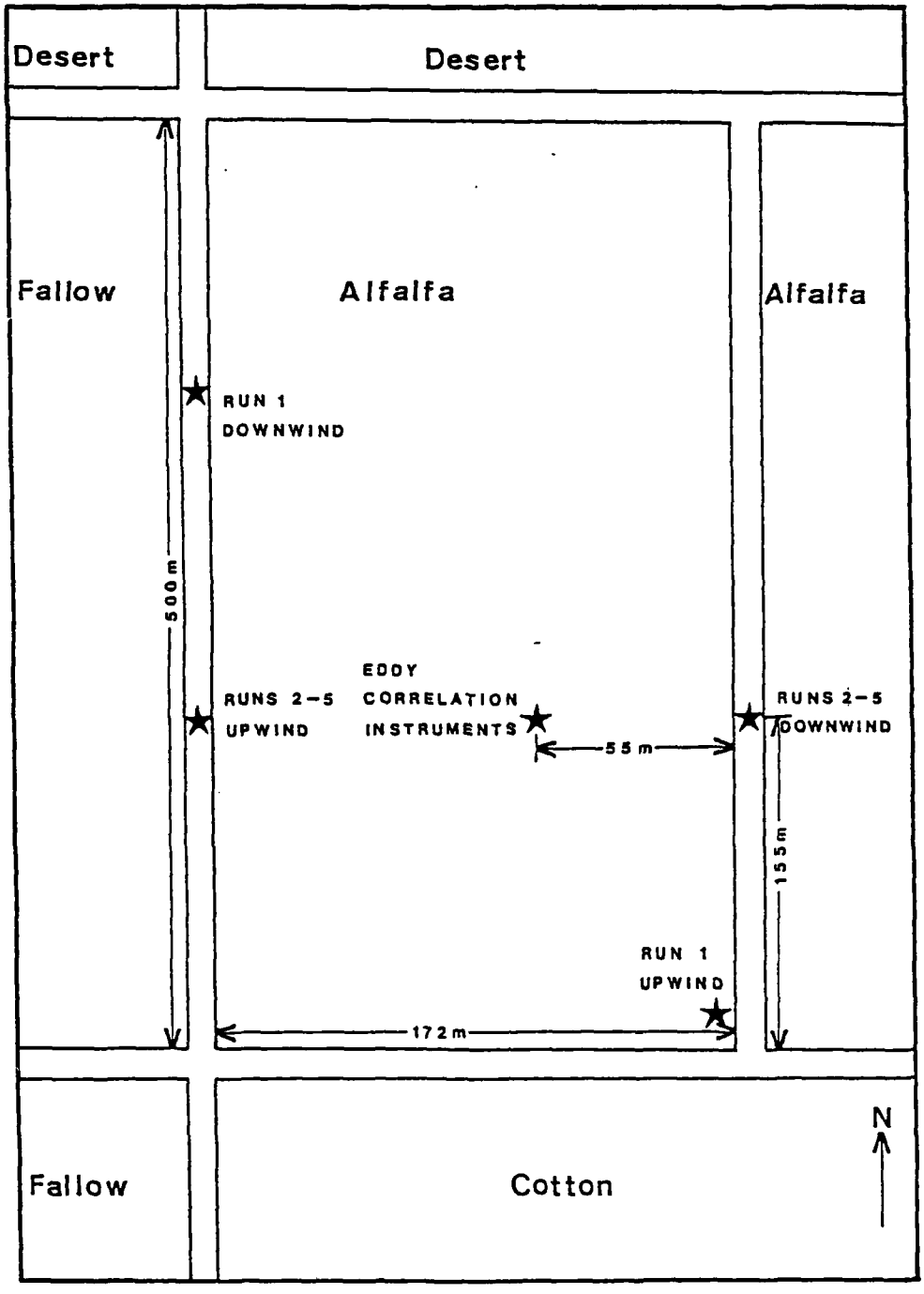

Fig. 5. Data collection locations at field site.

saturated with water vapor it contains only several percent moisture by weight. Therefore, the differences in upwind and downwind water vapor densities are relatively small. Because of this, the use of sensitive and accurate instrumentation was required. Since vertical profiles were obtained at several locations, the data collection system used was highly mobile.

Data were collected on dry and wet bulb temperatures, pressure, wind speed, and wind direction. A tethered balloon system with an airsonde package suspended beneath it (Fig. 6) was utilized for data collection. Data were transmitted to a receiver every six seconds (Fig. 7). The specifications for the sensors of the airsonde package were: temperature ± 0.5 °C, pressure ± 0.5 mb, wind direction ± 5.0 °, and wind speed ± 0.25 m sec^{-1}. The receiver in turn transferred the data to magnetic tape. Sequential observations to a height of 70 meters of both upwind and downwind profiles of the alfalfa field were taken during 30-minute periods along the same streamlines in mid-afternoon (1300 to 1700 MST). Observation sets were taken when the wind direction was steady. A total of five sets of balloon flights were considered acceptable for analysis. For all flights except for the first, upwind conditions consisted of a dry fallow field. The upwind conditions for the first run was a dry cotton field with less than 40 percent canopy coverage.

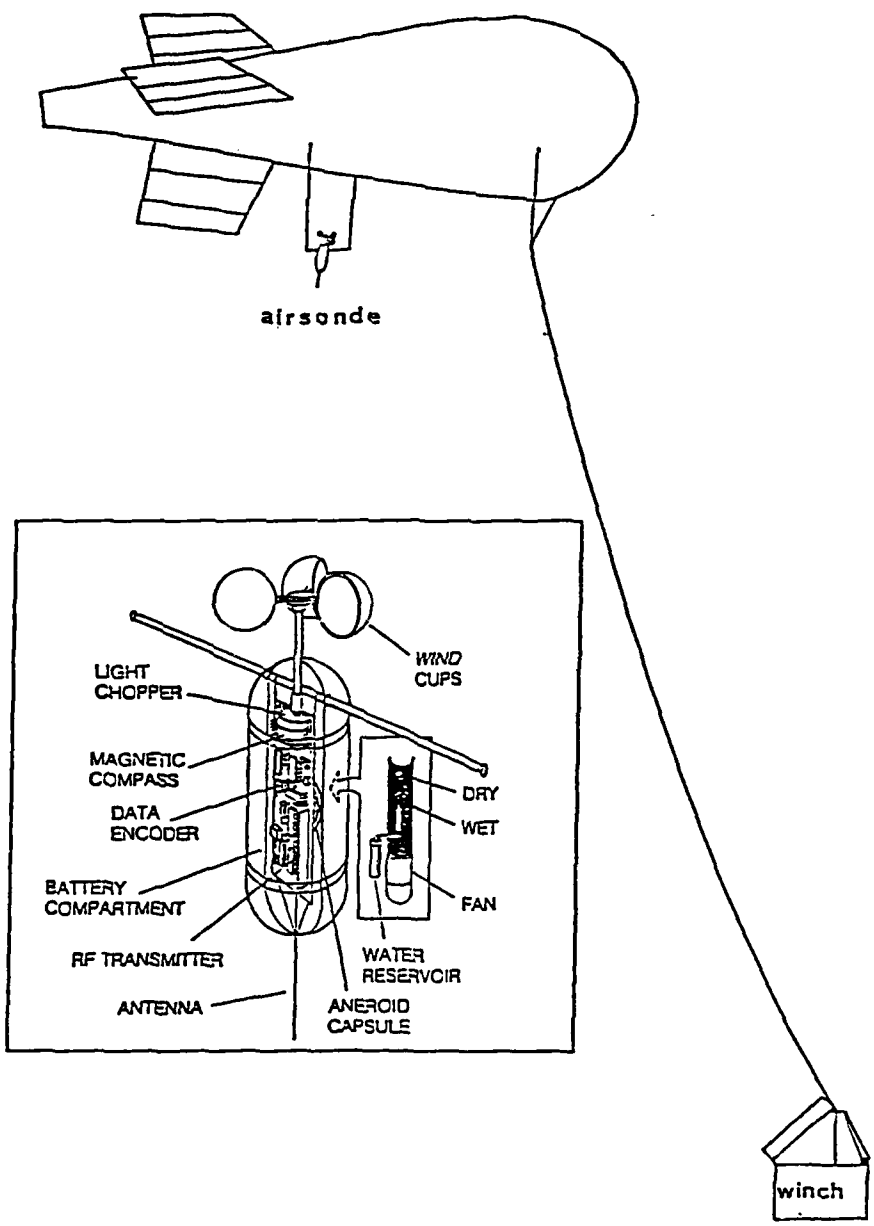

Fig. 6. Tethered balloon system with associated airsonde package and winch.

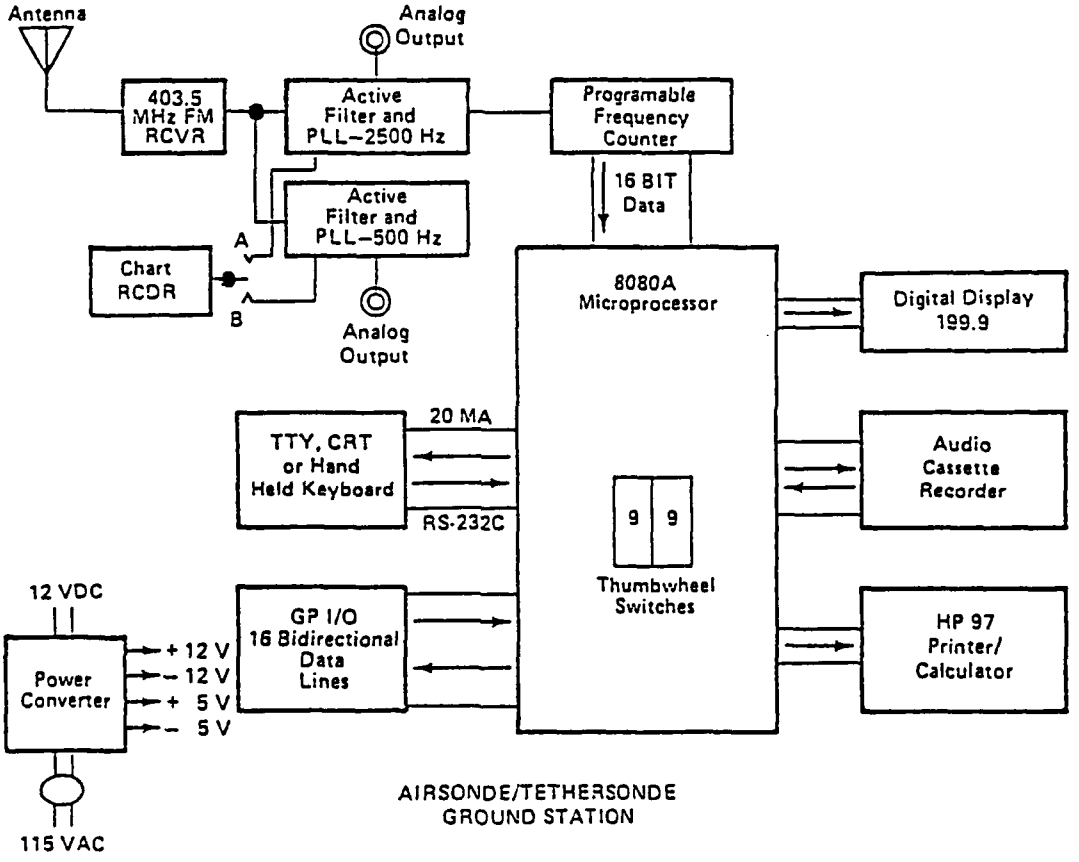

Fig. 7. Tethered balloon ground receiver station.

In order to assess the water-vapor budget estimates of evapotranspiration, independent estimates of the evapotranspiration rates along the same streamlines as the balloon flights were made using an eddy correlation system.

The eddy correlation method measures the flux of an atmospheric quantity directly by sensing the properties of turbulent eddies as they pass through a measurement level on an instantaneous basis (Oke, 1978). Fig. 8 depicts an example of the time series obtained using eddy correlation measurements.

The mean vertical flux of an entity in the atmosphere per unit mass is given by

$$F_c = \rho_a \overline{wc} \qquad [7]$$

Where F_c is the vertical flux of c, w the vertical velocity, and c an atmospheric entity. The overbar denotes an average value taken over a time period of suitable duration.

In the surface layer all entities in the atmosphere exhibit short-term fluctuations about their mean values (Fig. 8). Therefore, the instantaneous values of w, c, and ρ_a in [7] can be expressed as

$$w = \bar{w} + w', \; c = \bar{c} + c', \text{ and } \rho_a = \bar{\rho}_a + \rho_a' \qquad [8]$$

The primed quantities denote the instantaneous departures from the mean. Substituting the expressions of [8] into equation [7], neglecting the minor fluctuations in air

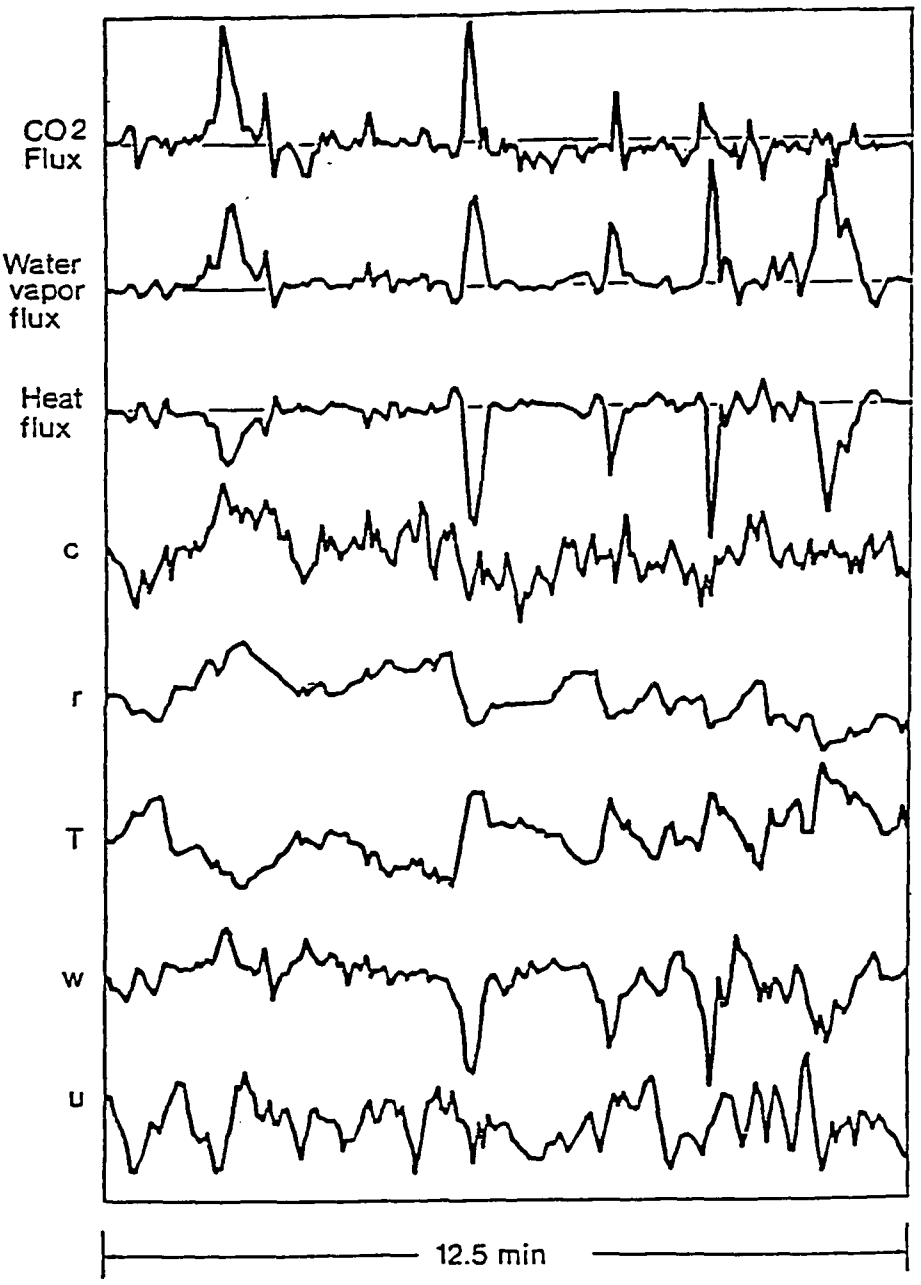

Fig. 8. Example time series of wind speed (u), vertical wind (w), temperature (T), water vapor mixing ration (r), CO_2 concentration, and fluxes of CO_2, heat, and water vapor as measured by eddy correlation.

density in the surface layer, and applying the rules of Reynolds averaging, equation [7] reduces to

$$F_c = \rho_a \overline{w}\,\overline{c} + \rho_a \overline{w'c'} \qquad [9]$$

The first term on the right hand side of equation [9] represents the flux of c due to the mean vertical flow. The second term represents the flux due to turbulent eddies. For a sufficiently long duration of time over a horizontally uniform surface, the total amount of ascending air is approximately equal to the total amount of descending air. This means that the mean value of the vertical velocity (w) is approximately zero. Therefore, equation [9] is simplified to

$$F_c = \rho_a \overline{w'c'} \qquad [10]$$

To collect the data a Campbell Scientific Instruments (CSI) krypton hygrometer and a one-dimensional sonic anemometer were placed near the center of the field at a height of 1 meter above the crop. This was well within the fully adjusted constant flux layer. This allowed for a maximum of fetch and ease of lining up the balloon observations along the same streamline. These instruments were connected to a CSI 21X micrologger that collected the data at 10 Hz. The voltage differential of the krypton hygrometer was measured and converted to q′ by the micrologger. w′ was measured by the sonic anemometer and also stored in the micrologger. The primed quantities, w′

and q', are the instantaneous departures of the mean of vertical windspeed and water vapor. The micrologger then calculated w'q' and computed evapotranspiration in W m^{-2} based on equation [10] as

$$ET = L \rho_a \overline{w'q'} \qquad [11]$$

Where ρ_a was 1.05 Kg m^{-3} and L is equal to 2.45×10^6 J Kg^{-1}. Twenty-minute averages of evapotranspiration were calculated.

Data Handling/Processing

The data from the tethered balloon flights were transferred from magnetic tape to floppy disk. These data were then grouped into data sets, consisting of upwind and downwind vertical profiles. For comparison of the profiles of temperature and specific humidity, the upwind data sets were paired with their corresponding downwind data sets, creating an upwind and downwind profile for each of the balloon flights. The data recorded during the ascent and descent of the balloon for a specific flight were merged and sorted by decreasing pressure values. This was necessitated by the fact that in order to obtain a coherent profile of temperature and specific humidity, the pressure values must be strictly decreasing with altitude. The pressure values obtained by the airsonde were not always strictly decreasing with height because the balloon and airsonde package, which was suspended below the balloon,

tended to bob up and down with gusts of wind, giving pressure readings that did not decrease monotonically with increasing height. Once this sorting was completed the data were processed to get virtual temperature (T_v), potential temperature (θ), saturated vapor pressure (e_s), vapor pressure (e_a), specific humidity (q), and the height of the airsonde above ground level (ZAGL). Potential temperature was calculated from Poisson's equation. The Goff-Gratch formula (equation [12]), taken from the Smithsonian Meteorological Tables (List, 1971), was used to obtain the saturated vapor pressure from the wet and dry bulb temperatures.

$$\text{Log}_{10}\, e_w = -7.90298(T_s/T-1) + 5.02808(\text{Log}_{10}(T_s/T)) \quad [12]$$
$$- 1.3816\text{x}10^{-7}(10^{11.344(1-T/T_s)}-1)$$
$$+ 8.1328\text{x}10^{-3}(10^{-3.49149(T_s/T-1)}-1) + \text{Log}_{10}e_{ws}$$

Where e_w is the saturation vapor pressure over a plane surface of pure ordinary liquid water (mb), T is the absolute temperature in degrees Kelvin, T_s is the steam point temperature (373.16 °K), and e_{ws} is the saturation vapor pressure of pure ordinary liquid water at steam point temperature (1 standard atmosphere = 1013.246 mb).

Actual vapor pressure was determined from the saturation vapor pressure at the wet bulb temperature using the famous psychometric equation

$$e_a = e_s(T_w) - \left[(P\ C_p)/(L\ \epsilon)\right](T - T_w) \quad [13]$$

Where P is the pressure in mb, ϵ the ratio of the mass of water to the mass of air (.622), the term $(T - T_w)$ the difference between the dry and wet bulb temperatures. C_p is 1004 J °K Kg^{-1} and L is 2.45×10^6 J Kg^{-1}. After determining e_a, specific humidity (q) was calculated by

$$q = \epsilon e_a / (P - .378 e_a) \qquad [14]$$

Where ϵ, e_a, and P have previously been defined.

To determine the heights at which the airsonde was sampling data, the integrated form of the Hydrostatic equation, sometimes called the Hypsometric formula, was used

$$\Delta Z = \left[(R_d T_{avg})/g\right]\left[\ln(P_1) - \ln(P_2)\right] \qquad [15]$$

Here g is acceleration due to gravity at the earth's surface (9.8 m sec^{-2}), R_d is the gas constant for dry air (287 J $°K^{-1}$ Kg^{-1}), T_{avg} the average virtual temperature (T_v) of the atmospheric layer, and P_1 and P_2 the pressure at the bottom and the top of the atmospheric layer, respectively.

Once the required values were calculated the raw potential temperature and specific humidity profiles were plotted as a function of height. This was done as a check to see if the profiles of temperature were lapse upwind and inverted downwind, that the specific humidity profiles were lapse both upwind and downwind, and to locate any data influenced by entrainment or any other environmental

factors. Only five flights were deemed acceptable for analysis. Upon inspection of these five raw profiles, it was found that the second run was influenced by a change in wind direction in which the upwind conditions consisted of irrigated cotton giving inverted upwind profiles. Data points collected when the wind direction was bad were discarded from the data file and the data set reprocessed. Some periods of minor entrainment were observed during runs 3 and 4, and the data that were obviously affected by this condition were removed from the profile.

Since any set of observations contains random errors as well as natural small-scale turbulent fluctuations, and since the data collected were instantaneous values and not temporal means, an objective analysis of the processed data was accomplished. This type of analysis has been defined as the "development and realization of methods which make it possible to use the measurement data of meteorological stations to reconstruct, objectively, the fields of meteorological elements of some type of regular network" (Gandin, 1965, p. 5). Objective analysis consists of removing the natural turbulent fluctuations within the data field, interpolating of data to obtain values on a grid, and then smoothing the resulting values at the grid points (Fritsch, 1969). A cubic spline smoothing technique developed by Kimball (1976) was used for reproducing the smooth mean vertical profiles of temperature and humidity for each run. This method subdivides each data set into

subranges by knots. Then a cubic polynomial is fitted to each subrange using a least squares method. A smooth curve with a smooth gradient is obtained because the first and second derivatives of each adjoining polynomial is made continuous at the knots. This technique allows the placement of knots wherever it seems the most appropriate. The method of knot placement as suggested by Kimball was followed and worked well. The cubic polynomials of each profile were then analytically integrated over the appropriate boundary conditions to yield the area between the upwind and downwind profiles. These integrated values of specific humidity and potential temperature represent the amount of water vapor input to the control volume from the surface and the amount of internal energy of the air transported to the crop and consumed in evapotranspiration, respectively.

Next the downwind data sets for the five runs were used to determine the average wind speed, fetch, and density of the parcel of air as it passed through the control volume. These values were calculated from the lower 15 to 20 meters of the profile depending on where the top of the enhanced water vapor layer or temperature inversion layer occurred.

RESULTS AND DISCUSSION

Ascents and descents were made sequentially, along the same streamline at the upwind and downwind edge of a well-watered alfalfa field on June 10, 11, 13, and 14, 1987. The data were collected under light-wind conditions of wind speeds between 1 to 5 m sec^{-1}. These data were used to reconstruct the vertical profiles of specific humidity and potential temperature at the leading and downwind edges of the alfalfa field. Modified water-vapor and internal energy methods were used to infer the amount of specific humidity input to the control volume from the surface and the portion of evapotranspiration from the crop due solely to sensible heat advection.

Observed Profiles

Specific Humidity

The specific humidity profiles for each run are depicted in Figs. 9 through 13 for June 10, 11, 13, and 14, respectively. Shown are the actual data points as well as the smoothed profiles. Lapse humidity conditions are evident in all profiles, with much stronger lapse conditions developing downwind of the leading edge. The distortions of the downwind profiles are a result of the input of water vapor into the control volume from the evapotranspiring crop. Turbulent eddies are responsible for transporting the evaporated water vapor upwards from

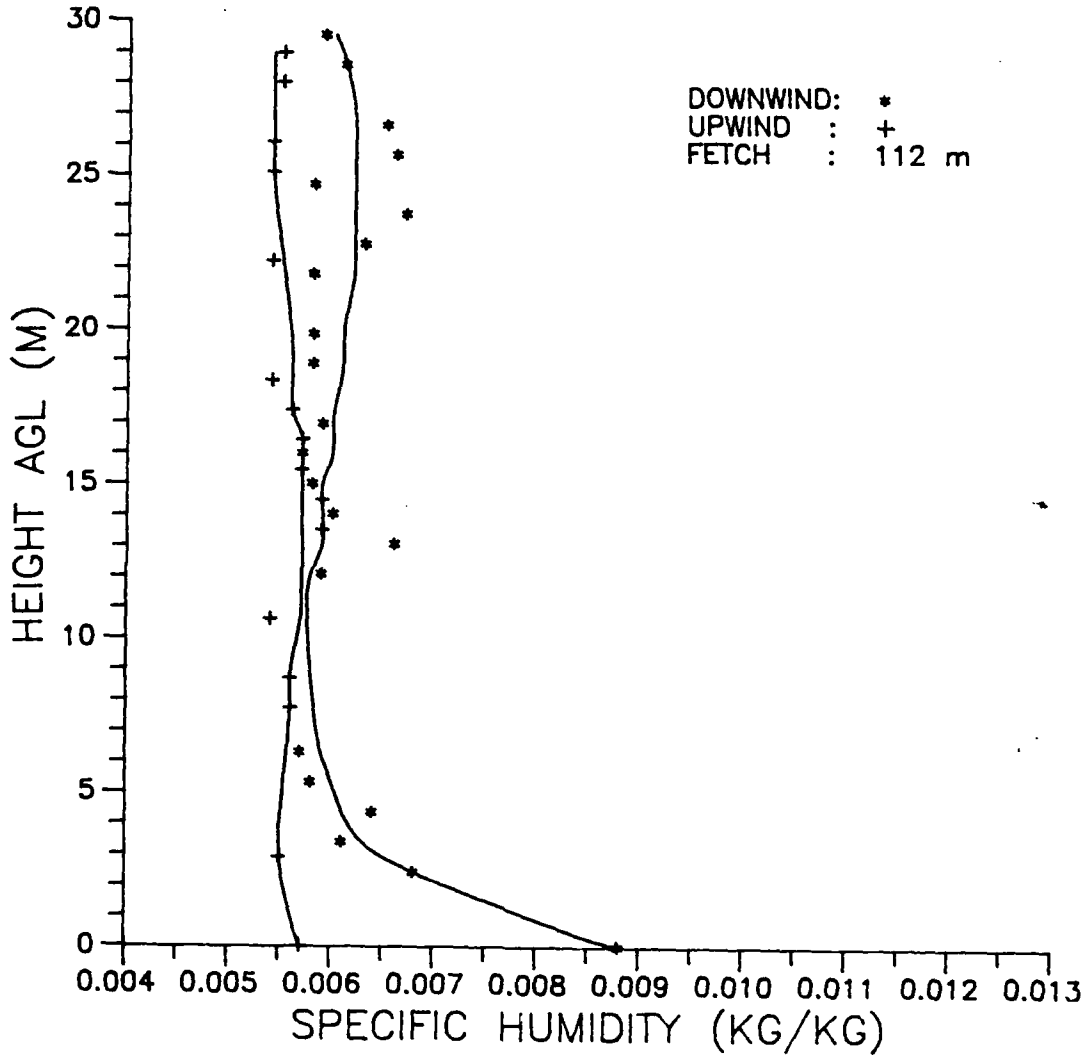

Fig. 9. Specific humidity profile for 10 June, 1987, 1330 MST.

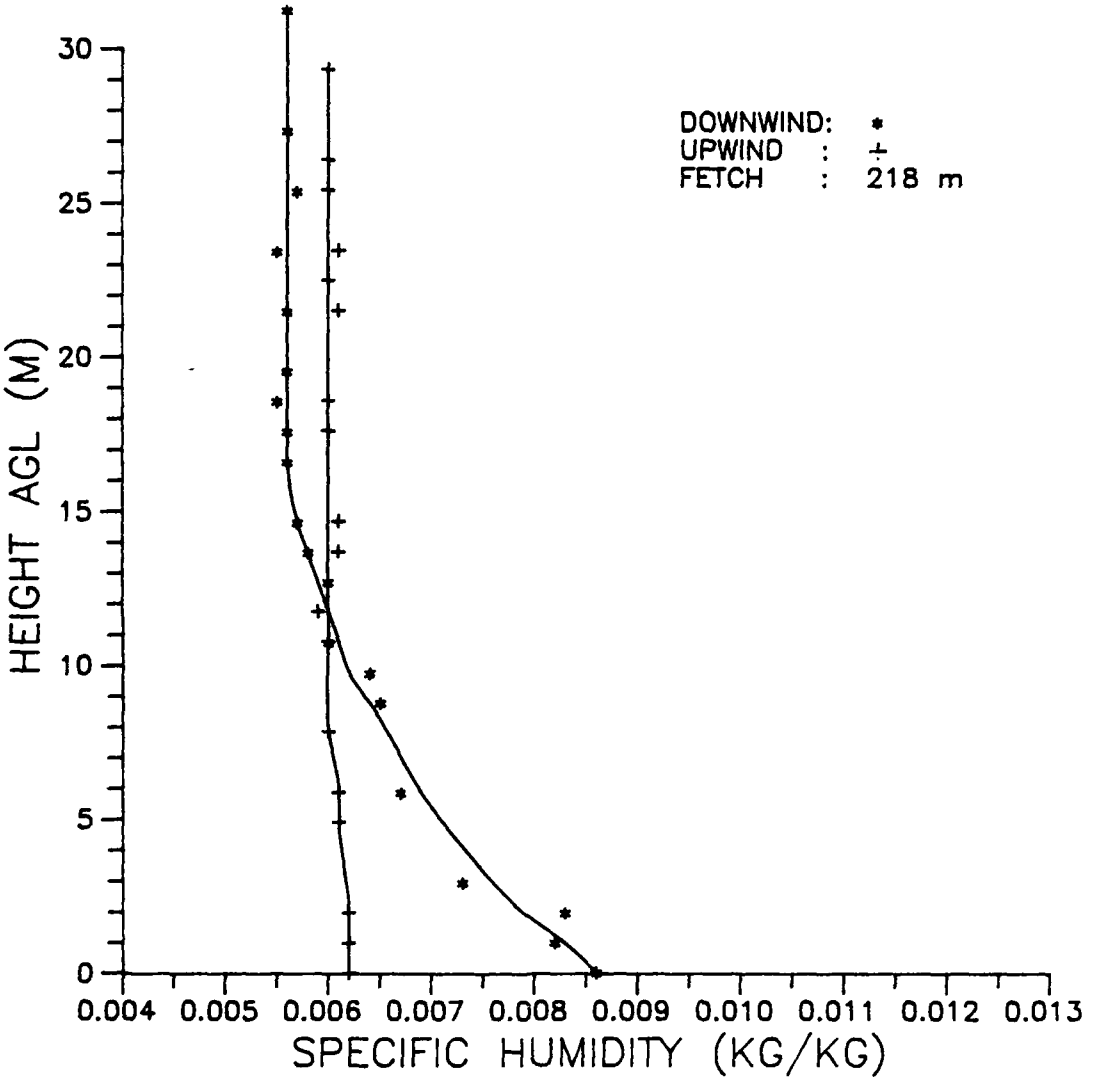

Fig. 10. Specific humidity profile for 10 June, 1987, 1530 MST.

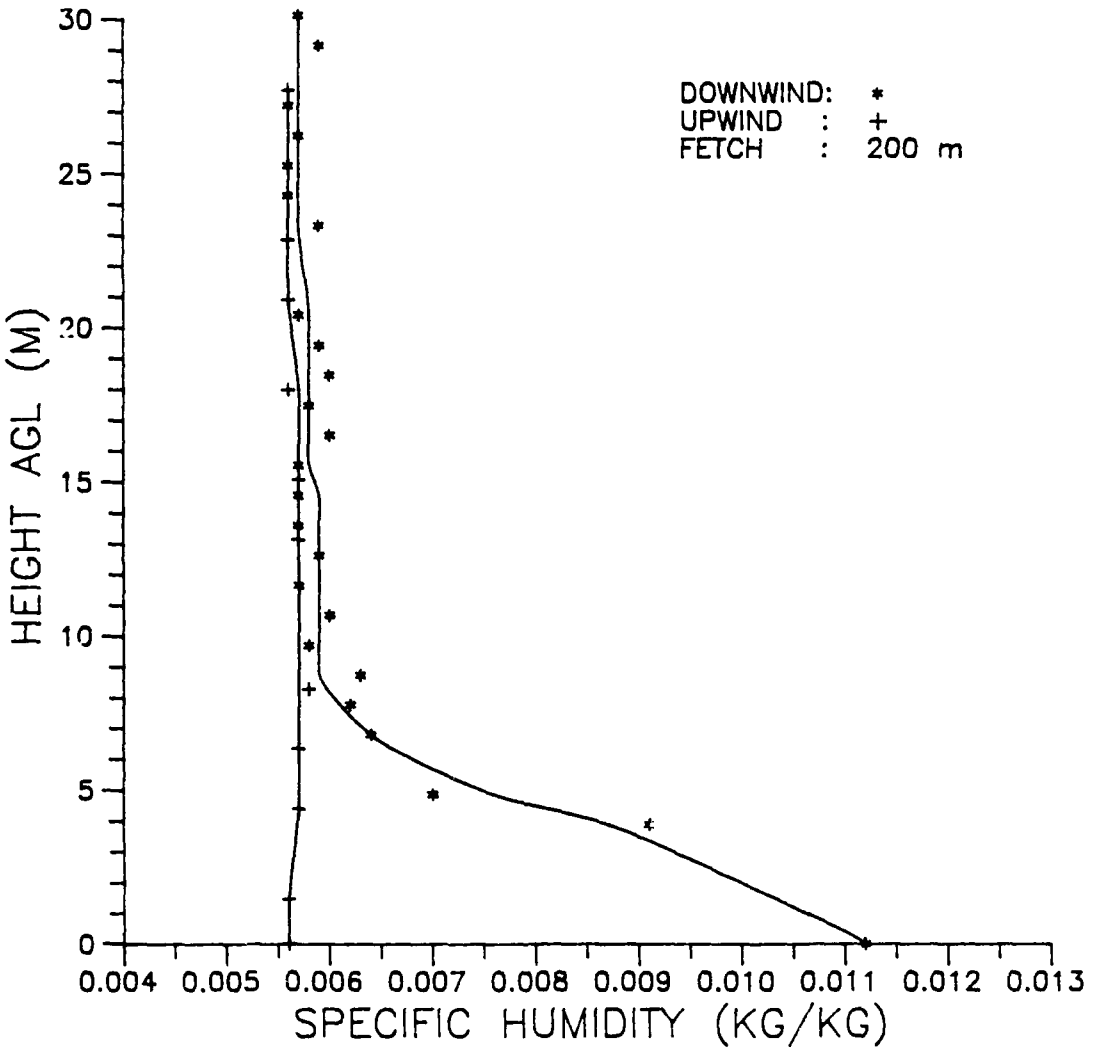

Fig. 11. Specific humidity profile for 11 June, 1987, 1620 MST.

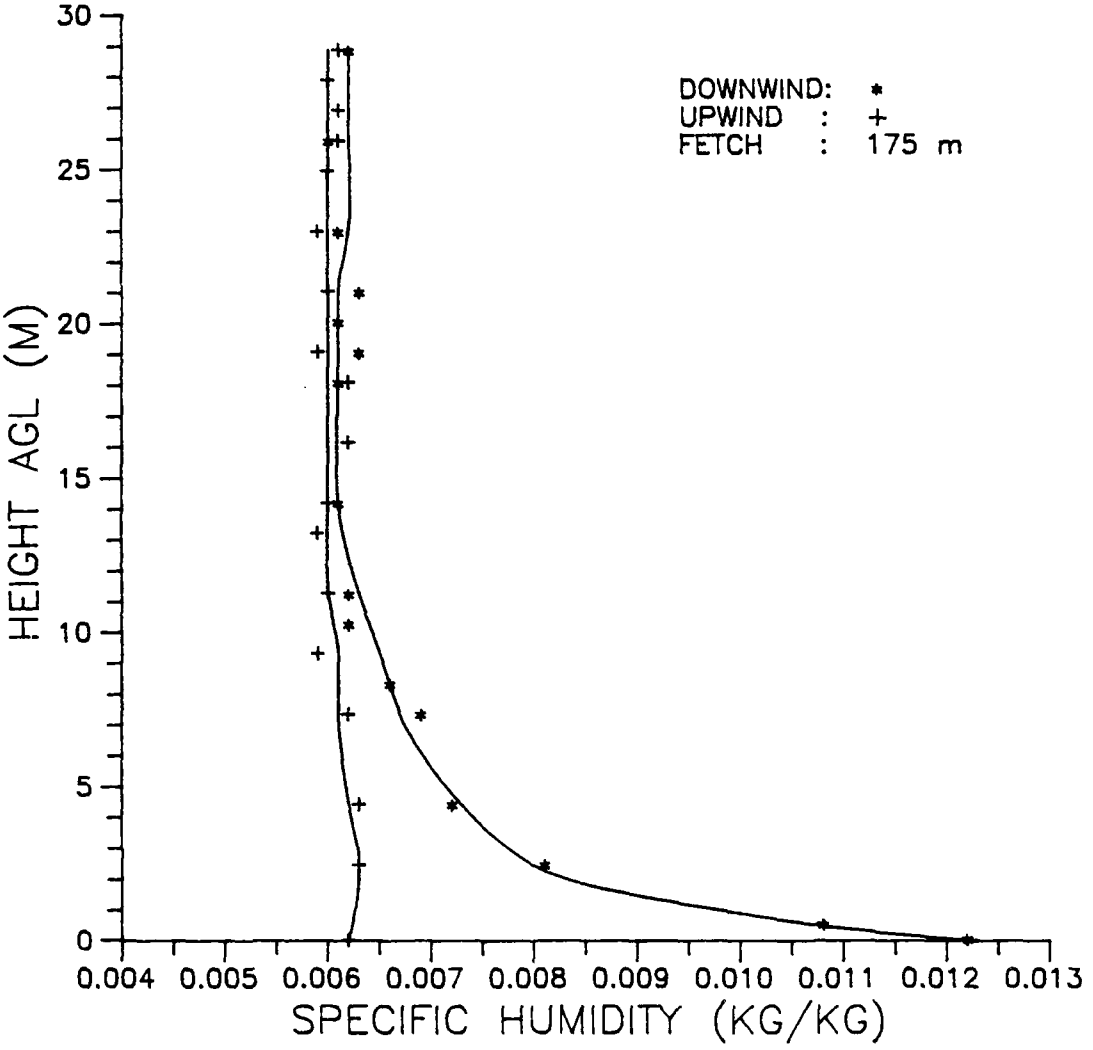

Fig. 12. Specific humidity profile for 13 June, 1987, 1620 MST.

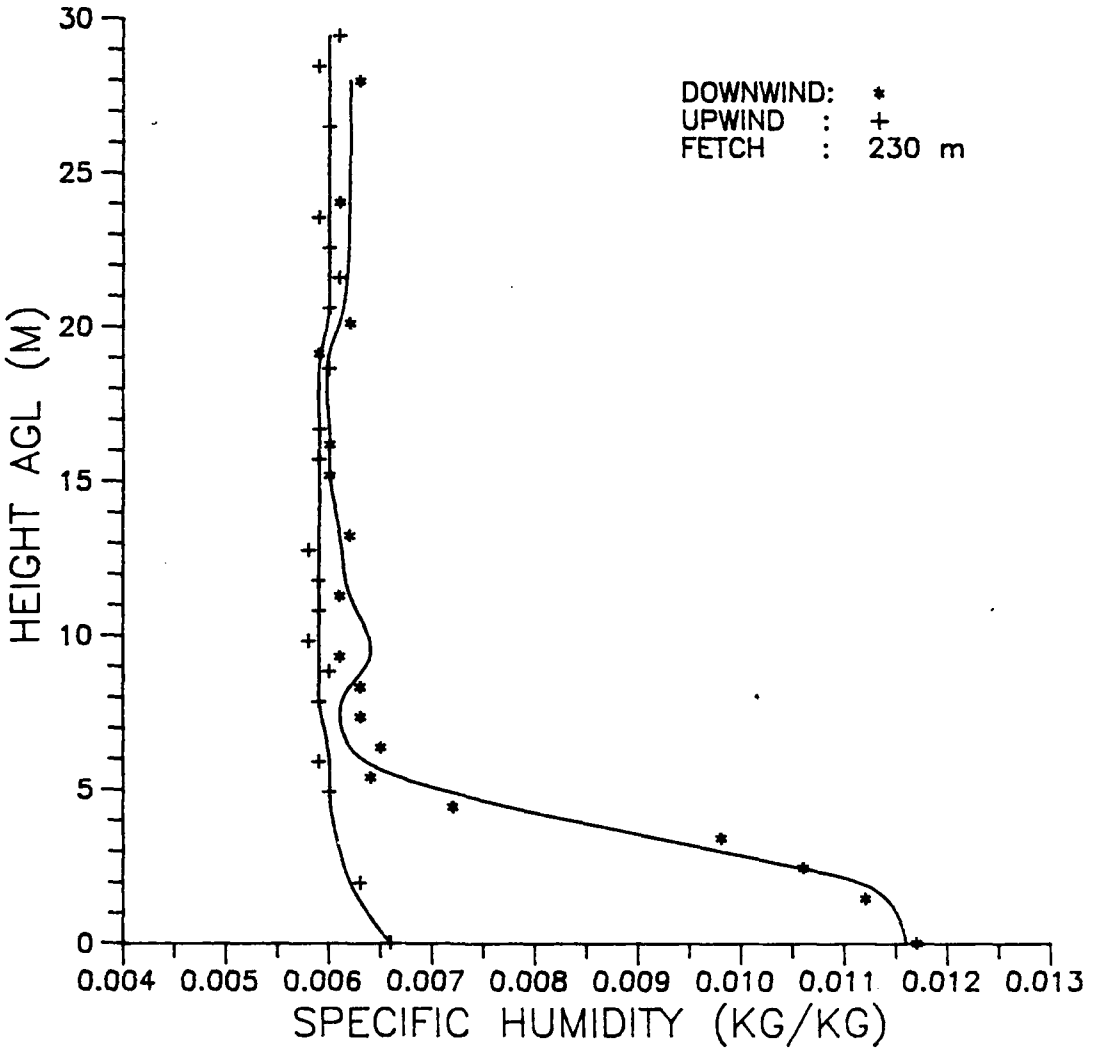

Fig. 13. Specific humidity profile for 14 June, 1987, 1540 MST.

the surface creating the enhanced water vapor layer. The depth of the enhanced water vapor layer that developed over the field varied from run to run, ranging from 5 meters to 12 meters. At these heights the differences between the upwind and downwind values of specific humidity are insignificant. The depth of the layer was proportional to the mean wind speed. As the mean wind speed increased, so did the height of the enhanced vapor layer. On average, the depth of air whose water vapor concentration was increased was about 10 meters. Note that these were primarily light-wind conditions.

As described previously the evapotranspiration rates for each run (ET) were estimated from equation [5]. Table 1 shows the comparison of the predicted results of equation [5] for each of the five runs, with the eddy correlation measured evapotranspiration rates for the corresponding days and times.

Fig. 14 presents these results on a 1:1 line. The predicted values show a close match with the measured values. An average deviation of approximately 7.2 percent was observed for all runs with an average deviation of 43.1 W m^{-2} from the actual evapotranspiration rate (ET). One must keep in mind that the eddy correlation estimates are not without error. This deviation was well within the uncertainty of ± 5% to 10% of the eddy correlation measurements. It is clear that this method, though fairly simple, has generated very accurate predictions for the

evapotranspiration rate in this study.

Table 1. Predicted evapotranspiration rates ($\overline{ET}$) using a modified vapor budget method vs. evapotranspiration rates as measured by eddy correlation (ET) for 10, 11, 13, and 14 June, 1987. Net radiation (Rn) values are 20 minute averages for an adjacent alfalfa field not recently watered.

RUN	DAY	TIME MST	ET (W/m^2)	$\overline{ET}$ (W/m^2)	Rn (W/m^2)
1	10	1330	608.3	673.0	649.1
2	10	1530	589.2	635.5	496.5
3	11	1620	439.5	430.9	371.0
4	13	1620	306.9	340.5	461.4
5	14	1540	540.3	582.1	546.4

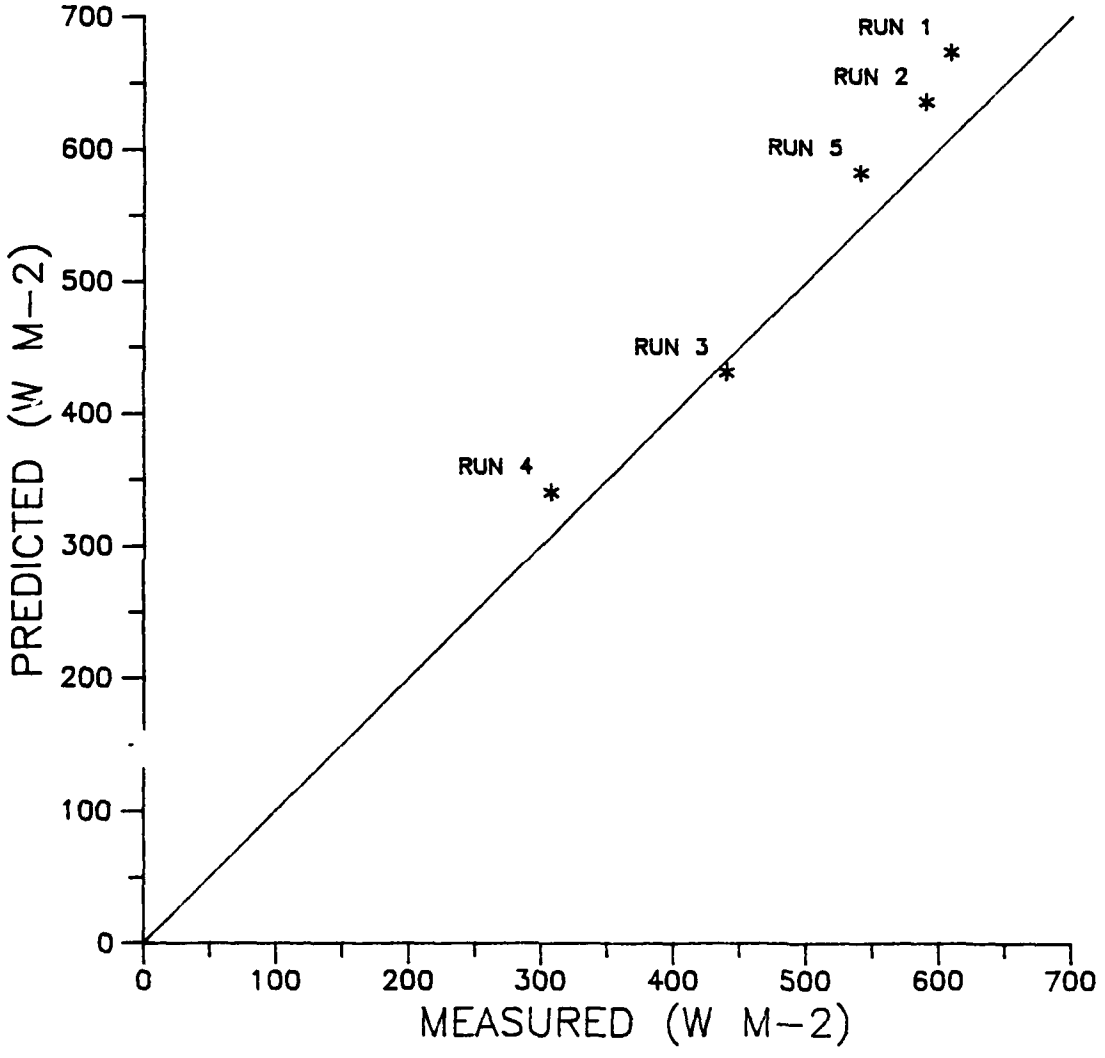

Fig. 14. Predicted versus measured evapotranspiration rates for runs 1 through 5.

Potential Temperature

The smoothed potential temperature profiles of the five runs are shown in Fig. 15 through 19 for June 10, 11, 13, and 14, respectively. All of the upwind profiles were lapse. This was to be expected for air originating over a dry, hot surface. The downwind profiles were all inverted. These profiles suggest a deep surface-inversion layer has developed over the field. The depth of this inversion layer is representative of the depth of the advected air which supplies sensible heat to the cooler evapotranspiring surface. As was seen for the water vapor, the height of the temperature inversion layer was related to the mean wind speed. As the mean wind speed increased, so did the inversion height. This height varied from 14 meters to 16 meters with an average depth of 15 meters. The decrease of air temperature at the surface was quite pronounced. For example, the fourth run on 13 June showed a decrease in air temperature of 7.2 °C as the parcel of air passed over the crop at 1 meter above ground level.

Table 2 compares the evapotranspiration rates due solely to advection (ET') calculated from equation [6], as well as the the total evapotranspiration rates measured the eddy correlation system. It is clear that significant amounts of energy used in evapotranspiration were supplied by the advection of sensible heat. It is demonstrated that horizontal advection contributed between 35 percent to 86 percent or an average of 301.4 W m^{-2} of the total

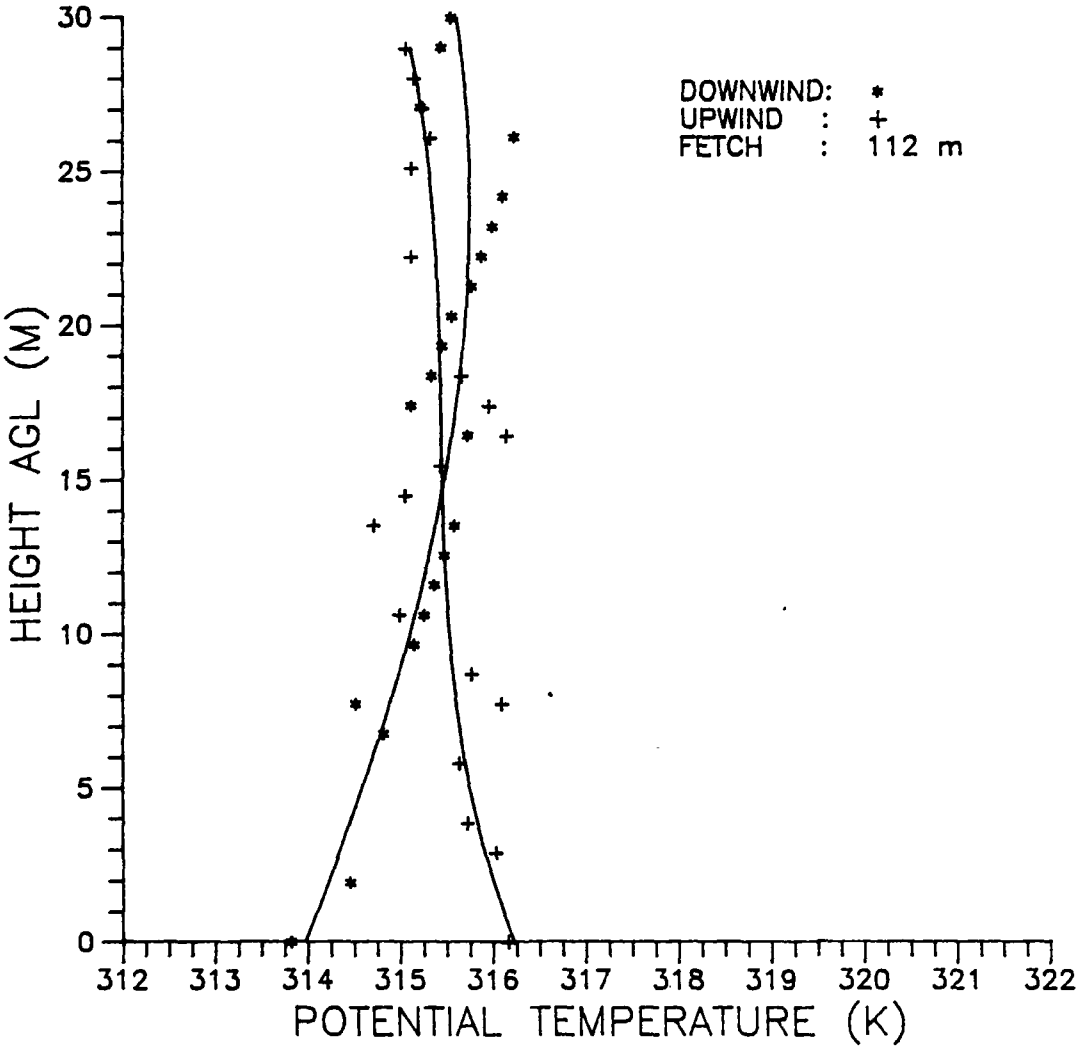

Fig. 15. Potential temperature profile for 10 June, 1987, 1330 MST.

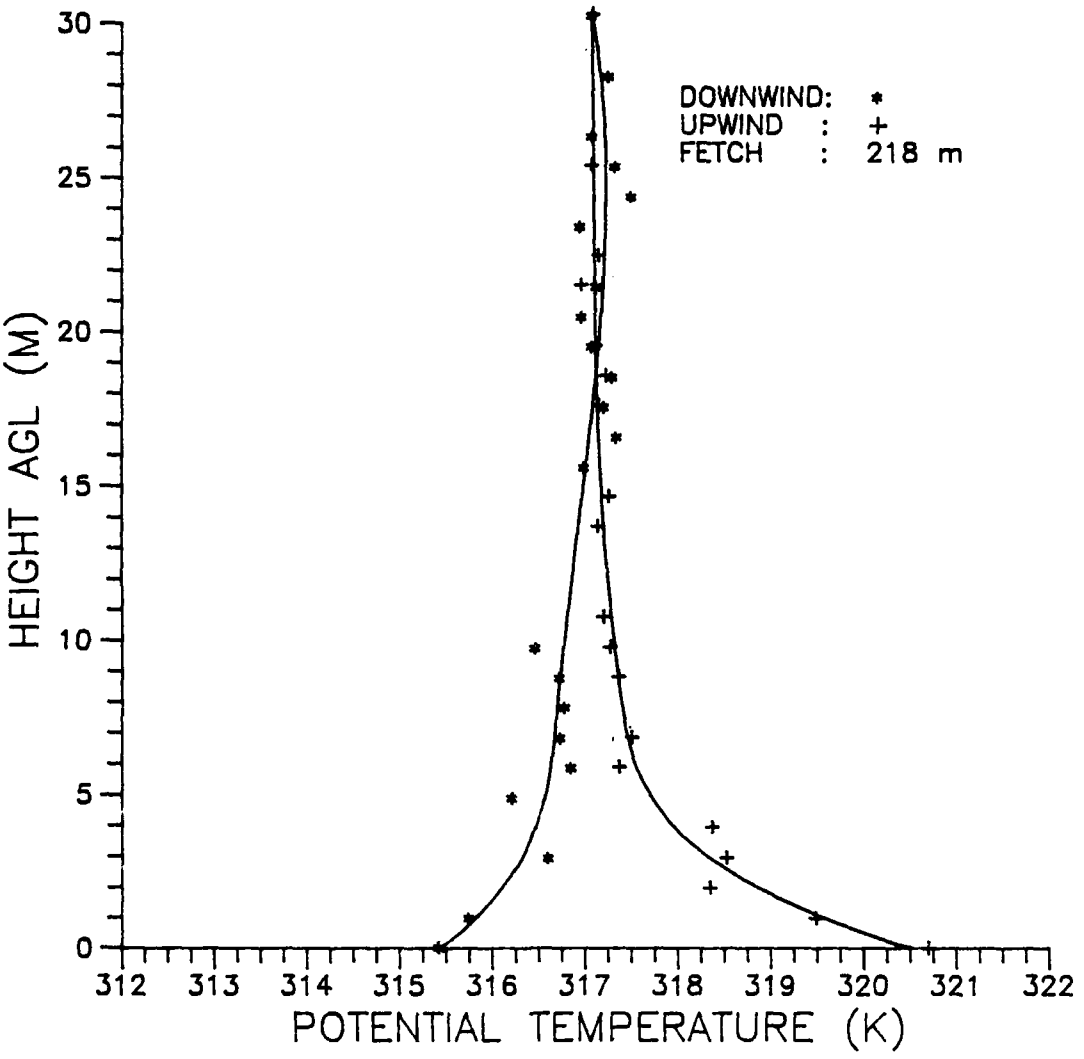

Fig. 16. Potential temperature profile for 10 June, 1987, 1530 MST.

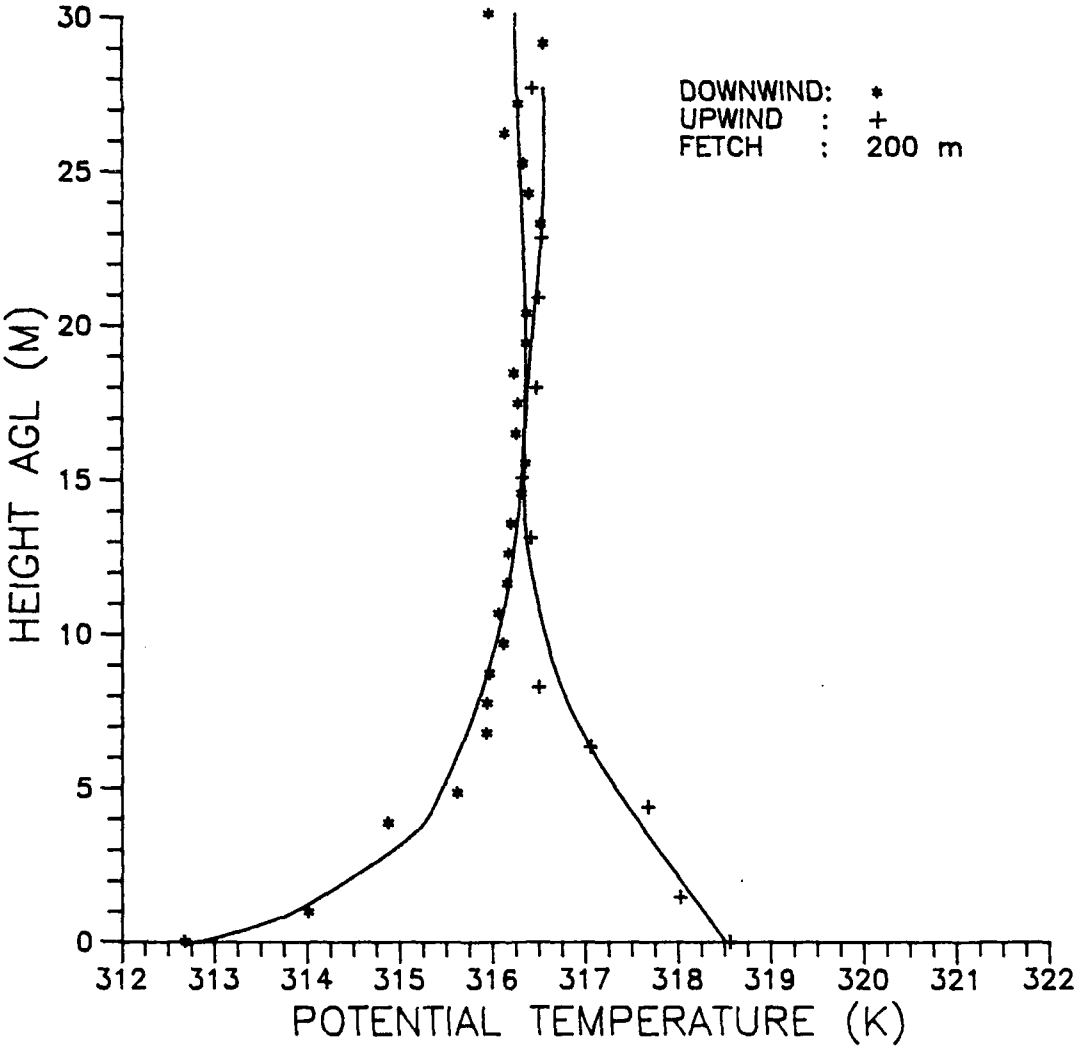

Fig. 17. Potential temperature profile for 11 June, 1987, 1620 MST.

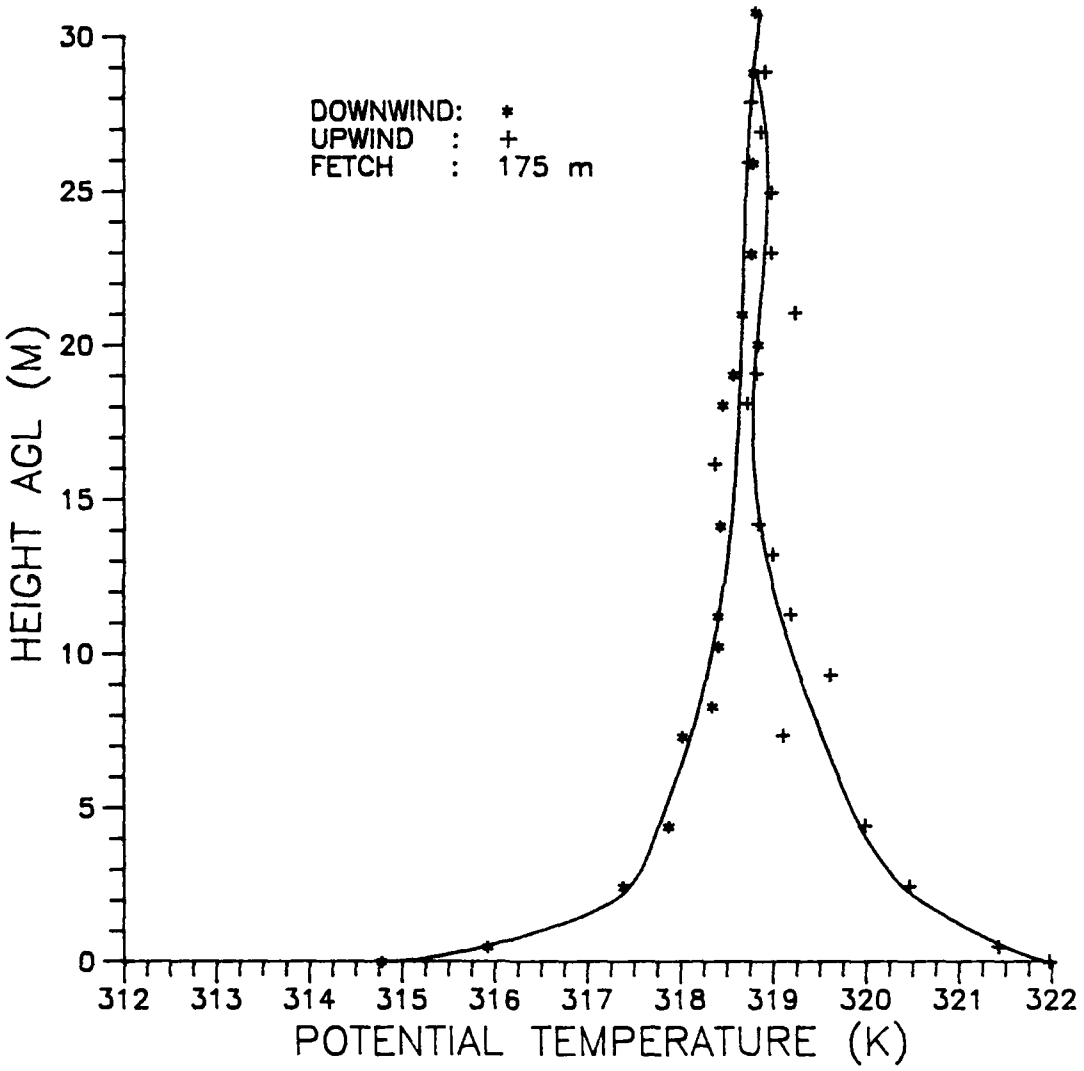

Fig. 18. Potential temperature profile for 13 June, 1987, 1620 MST.

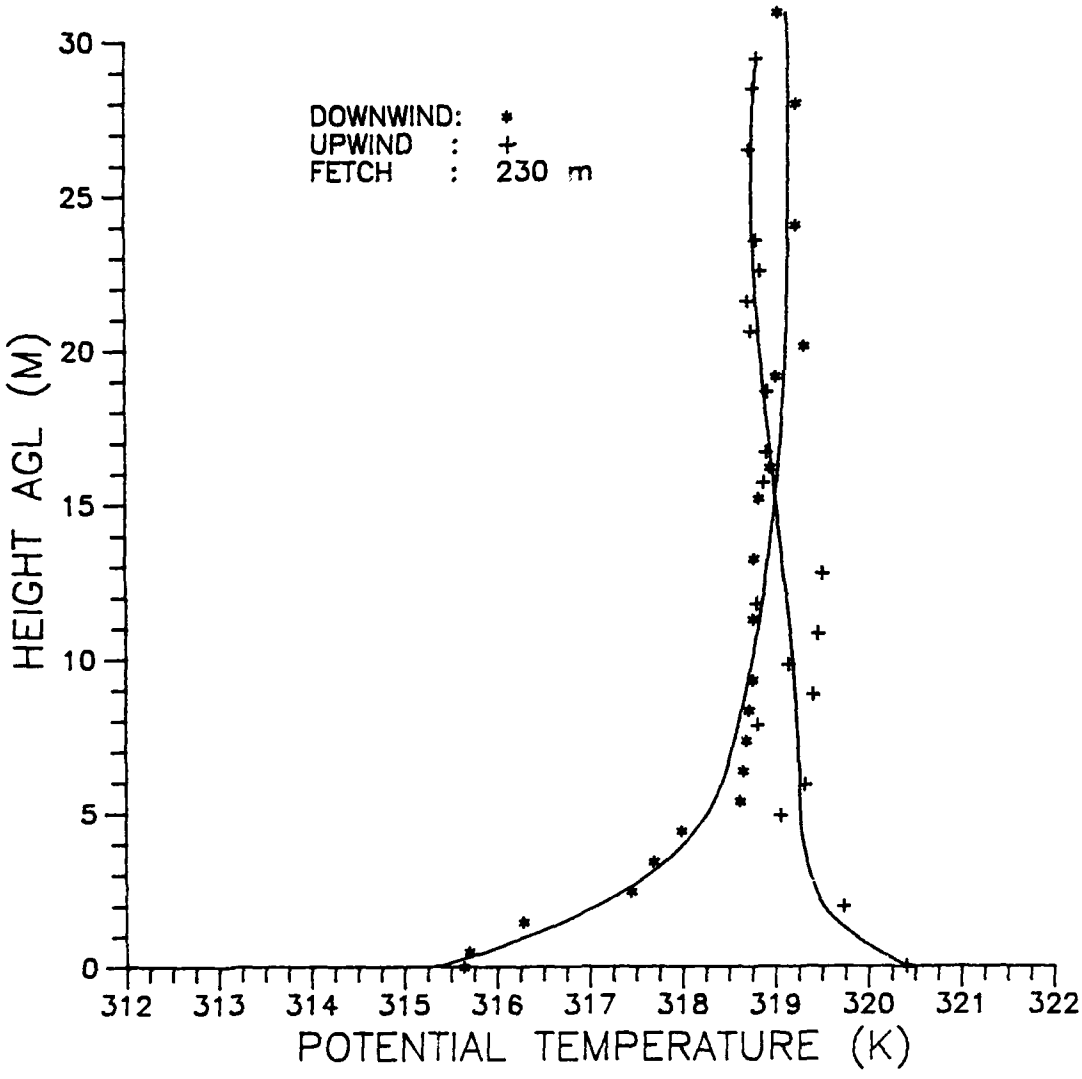

Fig. 19. Potential temperature profile for 14 June, 1987, 1540 MST.

evapotranspiration rate as measured by eddy correlation. This suggests that as the vertical temperature profile of a parcel of air is modified downwind of a leading edge, a deep layer of the lower atmosphere is supplying a significant amount of energy, through vertical transport, for use in evapotranspiration.

Table 2. Comparison of the estimated evapotranspiration rates (ET') due solely to the horizontal advection of sensible heat using a modified energy budget method with evapotranspiration rates measured by eddy correlation for 10, 11, 13, and 14 June, 1987. Net radiation (Rn) values are 20 minute averages for an adjacent alfalfa field not recently watered.

RUN	DAY	TIME MST	ET (W/m^2)	ET' (W/m^2)	% of ET	Rn (W/m^2)
1	10	1330	608.3	452.6	74	649.1
2	10	1530	589.2	437.4	74	496.5
3	11	1620	439.5	155.2	35	371.0
4	13	1620	306.9	263.1	86	461.4
5	14	1540	540.3	198.9	37	546.4

These results compare well with those obtained by other methods of measuring evapotranspiration due to advection (Hanks et al., 1971; Brakke et al., 1978).

A comparison of the heights of the enhanced vapor layer with the heights of the temperature inversion is of interest. As the height of the temperature inversions increased so did the heights of the enhanced water vapor layers. However, the temperature inversion heights, in all cases, appeared slightly greater than those of the enhanced vapor layer.

SUMMARY AND CONCLUSIONS

Specific humidity and potential temperature profiles were measured to a height of 70 meters at the leading and downwind edges of a well-watered alfalfa field, during conditions of horizontal sensible heat advection. An eddy correlation system made independent measurements of evapotranspiration along the same streamline as the upwind and downwind locations.

As the parcels of air moved across the alfalfa field, the profiles of specific humidity became increasingly lapse. This change reflects the upward flux of latent heat in the lower atmosphere. Evapotranspiration values were predicted from the downwind distortion of specific humidity profiles using a vapor-budget technique. These estimates agreed very well with measured evapotranspiration rates from the eddy correlation system. The deviation between predicted and measured values was approximately 7.2 percent or 43.1 W m^{-2} for all five runs. The depth of the enhanced water vapor layer averaged about 10 meters for the five runs, during light-wind conditions. The evapotranspiration rates can be inferred with good accuracy from the upwind and downwind profiles of specific humidity, if those measurements are made to an adequate height.

The vertical profiles of potential temperature exhibited a developing inversion layer as the parcels of air moved across the field. This change in temperature

reflected the downward flux of sensible heat taken from the advected air for use by the crop in evapotranspiration. The rates of evapotranspiration due solely to advection were calculated from the modifications of the vertical profiles using an internal energy method. The advected energy appears to have contributed between 35 percent and 86 percent of the total evapotranspiration rate. The depth of the inversion layer which developed over the irrigated crop was approximately 15 meters for all runs during light-wind conditions.

It has been shown in previous studies that the advection of sensible heat can greatly enhance evapotranspiration and reduce water-use efficiency. The results of this study show two things. First, that a modified vapor-budget method can accurately estimate the short-term rates of evapotranspiration from the measurement of the upwind and downwind profiles of humidity. Secondly, that the amount of evapotranspiration due solely to advection can be calculated from the upwind and downwind profiles of temperature. However, these profiles must be measured to a great enough depth. This approach is more simple and direct than previous approaches. These results are similar to previous works (Hanks et al. 1971; Brakke et al. 1978) which indicate that advection is responsible for a large portion of evapotranspiration in arid regions.

REFERENCES

Abdel-Aziz, M.H., S.A. Taylor, and G.L. Ashcroft. 1964. Influence of advective energy on transpiration. Agron. J. 56:139-142.

Baldocchi, D.D., S.B. Verma, and N.J. Rosenberg. 1981. Environmental effects on the CO_2 flux and CO_2 water flux ratio of alfalfa. Agric. For. Meteorol. 24: 175-184.

Brakke, T.W., S.B. Verma, and N.J. Rosenberg. 1978. Local and regional components of sensible heat advection. J. Appl. Meteorol. 17:955-963.

Blad, B.L. and N.J. Rosenberg. 1974. Lysimetric calibration of the bowen-ratio energy balance method for evapotranspiration estimation in the central Great Plains. J. Appl. Meteorol. 13:227-235.

Dyer, A.J. and T.V. Crawford. 1965. Observations of the modification of the microclimate at a leading edge. Quart. J. Roy. Meteorol. Soc. 91:345-349.

Fritsch, J.M. 1969. Objective analysis of a two dimensional data field by the cubic spline technique. Atmospheric Science Paper #143. Department of Atmospheric Sciences, Colorado State University, 38 pp.

Gandin, L.S. 1965. Objective analysis of meteorological fields. U.S. Department of Commerce, Clearing House for Federal Scientific and Technical Information, N66-18047.

Hamlyn, J.G. 1983. Plants and microclimate. Cambridge University Press, N.Y. 323 pp.

Hanks, R.J., L.H. Allen, and H.R. Gardner. 1971. Advection and evapotranspiration of wide-row sorghum in the central Great Plains. Agron. J. 63:520-527.

Hipps, L.E., M. Agulto, and G.L. Wooldridge. 1988. A study of the atmospheric layer modified by an evaporating surface during conditions of horizontal advection of sensible heat. I. Observations. II. Analysis of turbulence diffusivities. Submitted to Boundary-Layer Meteorol., August 1987.

Huschke, R.E., ed. 1959. Glossary of meteorology, 2ed. American Meteorological Society, Boston, MA. 637 pp.

Inmula, P. and B.L. Sill. 1985. Measurement of irrigation evaporation losses by a new vapor budget technique. Technical Completion Report G-868-04, G-932-04, Water Resources Research Institute, Clemson University, S.C. 100 pp.

Kimball, B.A. 1976. Smoothing data with cubic splines. Agron. J. 68:126-129.

Lang, A.R.G. 1973. Measurement of evapotranspiration in the presence of advection by means of a modified energy balance procedure. Agric. Meteorol. 12:75-81.

List, R.J. 1971. Smithsonian meteorological tables, 6th edition. Smithsonian Institute Press, Washington DC. 527 pp.

Motha, R.P., S.B. Verma, and N.J. Rosenberg. 1979. Turbulence under conditions of sensible heat advection. J. Appl. Meteorol. 18:467-473.

Oke, T.R. 1978. Boundary Layer Climates. Metheun and Company, Ltd., N.Y. 372 pp.

Philip, J.R. 1959. The theory of local advection. J. Meteorol. 16:535-547.

Rao, K.S., J.C. Wyngarrd, and O.R. Cote 1974a. The structure of the two-dimensional boundary layer over a sudden change of surface roughness. J. Atmos. Sci. 31:738-746.

Rao, K.S., J.C. Wyngarrd, and O.R. Cote 1974b. Local advection of momentum, heat, and moisture in micrometeorology. Boundary-Layer Meteorol. 7:331-348.

Rider, N.E., J.R. Philip, and E.F. Bradley. 1963. The horizontal transport of heat and moisture - a micrometeorological study. Quart. J. Roy. Meteorol. Soc. 89:507-531.

Rosenberg, N.J. 1969. Advection of energy utilized in evapotranspiration by alfalfa in the east central Great Plains (U.S.A.). Agric. Meteorol. 6:19-184.

Rosenberg, N.J. and S.B. Verma. 1978. Extreme evapotranspiration by irrigated alfalfa: a consequence of the 1976 midwestern drought. J. Appl. Meteorol. 17(7):934-941.

Taylor, P.A. 1970. A model of airflow above changes in surface heat flux, temperature and roughness for neutral and unstable conditions. Boundary-Layer Meteorol. 1:1-39.

Taylor, P.A. 1971. Airflow above change in surface heat flux, temperature and roughness; an extension to include the stable case. Boundary-Layer Meteorol. 1:474-497.

Verma, S.B., N.J. Rosenberg, and B.L. Blad. 1978. Turbulent exchange for sensible heat and water vapor under advective conditions. J. Appl. Meteorol. 17:330-338.

APPENDIX

Data Listing Of The Lower 30 Meters Of The Vertical Profiles Of Potential Temperature And Specific Humidity For All Runs

Table A-1. Upwind data of ZAGL, potential temperature, pressure, wind speed, and wind direction for run 1, 10 June, 1987, 1330 MST.

ZAGL (m)	θ °K	P mb	Wind Speed m/s	Wind Direction °
.00	316.16	946.90	4.10	105.00
2.90	316.03	946.30	2.52	100.30
3.86	315.72	946.20	4.11	105.90
5.80	315.63	946.00	3.71	88.30
7.73	316.09	945.80	3.70	87.60
8.69	315.76	945.70	1.70	170.00
10.62	314.98	945.50	3.18	83.30
13.51	314.71	945.20	6.48	101.00
14.48	315.05	945.10	6.58	97.10
15.44	315.43	945.00	5.61	97.20
16.41	316.14	944.90	1.70	169.00
17.38	315.95	944.80	1.90	183.00
18.34	315.65	944.70	1.80	162.00
22.21	315.11	944.30	4.20	127.90
25.10	315.11	944.00	1.40	165.00
26.07	315.32	943.90	2.40	192.00
27.03	315.23	943.80	4.38	152.80
28.00	315.14	943.70	2.10	166.00
28.96	315.05	943.60	3.20	188.00

Table A-2. Downwind data of ZAGL, potential temperature, pressure, wind speed, and wind direction for run 1, 10 June, 1987, 1330 MST.

ZAGL (m)	θ °K	P mb	Wind Speed m/s	Wind Direction °
.00	313.81	944.90	2.50	138.00
1.93	314.45	944.50	2.20	129.00
6.75	314.81	944.00	3.70	153.00
7.72	314.51	943.90	2.50	134.00
9.65	315.14	943.70	2.20	152.00
10.61	315.25	943.60	2.20	138.00
11.58	315.36	943.50	1.60	.00
12.55	315.47	943.40	2.20	178.00
13.51	315.58	943.30	1.50	177.00
16.42	315.72	943.00	4.30	142.00
17.38	315.11	942.90	5.10	151.00
18.35	315.33	942.80	5.90	144.00
19.32	315.44	942.70	5.40	139.00
20.29	315.55	942.60	8.10	117.00
21.25	315.76	942.50	5.20	172.00
22.22	315.87	942.40	2.70	166.00
23.19	315.99	942.30	5.90	194.00
24.16	316.10	942.20	5.90	194.00
26.10	316.22	942.00	3.60	161.00
27.07	315.21	941.90	6.60	157.00
29.00	315.43	941.70	5.20	161.00
29.97	315.54	941.60	3.20	158.00

Table A-3. Upwind data of ZAGL, potential temperature, pressure, wind speed, and wind direction for run 2, 10 June, 1987, 1530 MST.

ZAGL (m)	θ °K	P mb	Wind Speed m/s	Wind Direction °
.00	320.70	939.80	.79	145.00
.98	319.48	939.60	2.81	138.20
1.96	318.34	939.50	5.04	19.40
2.94	318.52	939.40	6.50	20.80
3.92	318.36	939.30	3.45	14.80
5.88	317.36	939.10	4.01	11.60
6.85	317.50	939.00	4.30	38.80
8.81	317.35	938.80	4.58	8.60
9.78	317.26	938.70	8.66	14.60
10.76	317.19	938.60	4.01	281.90
13.69	317.13	938.30	2.26	6.00
14.66	317.25	938.20	3.47	6.40
17.59	317.14	937.90	2.86	336.00
18.57	317.22	937.80	2.42	24.10
19.54	317.10	937.70	3.60	343.80
21.50	316.95	937.50	3.83	15.10
22.47	317.14	937.40	3.33	336.40
25.40	317.06	937.10	3.11	342.50
30.28	317.07	936.60	4.61	11.10

Table A-4. Downwind data of ZAGL, potential temperature, pressure, wind speed, and wind direction for run 2, 10 June, 1987, 1530 MST.

ZAGL (m)	θ °K	P mb	Wind Speed m/s	Wind Direction °
.00	315.42	941.20	2.21	200.50
.97	315.74	941.00	1.26	126.60
2.91	316.59	940.80	3.70	41.80
4.86	316.20	940.60	5.40	166.90
5.83	316.84	940.50	7.22	153.60
6.80	316.72	940.40	5.08	212.80
7.78	316.77	940.30	4.63	193.00
8.75	316.71	940.20	5.29	214.10
9.72	316.45	940.10	6.70	162.10
15.56	316.98	939.50	5.64	206.40
16.54	317.33	939.40	7.47	180.00
17.52	317.19	939.30	5.23	192.90
18.49	317.28	939.20	5.43	206.30
19.47	317.06	939.10	5.15	198.40
20.44	316.95	939.00	4.60	206.80
21.42	317.11	938.90	4.60	180.00
23.37	316.93	938.70	4.52	186.80
24.34	317.48	938.60	4.40	222.50
25.32	317.31	938.50	4.53	180.20
26.29	317.06	938.40	4.72	180.00
28.24	317.24	938.20	4.92	224.00
30.20	317.06	938.00	5.10	188.70

Table A-5. Upwind data of ZAGL, potential temperature, pressure, wind speed, and wind direction for run 3, 11 June, 1987, 1620 MST.

ZAGL (m)	θ °K	P mb	Wind Speed m/s	Wind Direction °
.00	318.56	944.00	4.20	99.60
1.46	318.02	943.70	4.12	142.20
4.38	317.67	943.40	5.76	143.00
6.33	317.05	943.20	5.41	135.20
8.27	316.49	943.00	4.42	144.00
13.12	316.41	942.50	4.57	142.90
15.06	316.32	942.30	2.81	134.10
17.97	316.47	942.00	3.18	146.60
20.89	316.49	941.70	2.14	142.10
22.83	316.52	941.50	2.49	157.20
27.69	316.42	941.00	4.69	148.10

Table A-6. Downwind data of ZAGL, potential temperature, pressure, wind speed, and wind direction for run 3, 11 June, 1987, 1620 MST.

ZAGL (m)	θ °K	P mb	Wind Speed m/s	Wind Direction °
.00	312.68	941.90	1.94	97.20
.97	314.01	941.70	1.28	141.80
3.87	314.87	941.40	2.33	131.60
4.84	315.62	941.30	2.37	128.60
6.78	315.93	941.10	3.08	96.90
7.75	315.94	941.00	2.67	107.20
8.72	315.96	940.90	2.16	137.40
9.69	316.11	940.80	1.73	79.80
10.66	316.06	940.70	3.79	94.00
11.63	316.15	940.60	1.95	93.30
12.60	316.17	940.50	3.62	99.60
13.57	316.20	940.40	1.51	116.40
14.55	316.31	940.30	1.95	129.10
15.52	316.35	940.20	2.21	119.30
16.49	316.25	940.10	3.37	96.90
17.46	316.27	940.00	2.24	127.70
18.43	316.22	939.90	3.27	97.90
19.40	316.36	939.80	4.12	91.90
20.38	316.36	939.70	2.64	117.40
23.29	316.51	939.40	3.48	96.80
24.27	316.38	939.30	1.90	122.80
25.24	316.32	939.20	2.59	134.70
26.21	316.12	939.10	.98	109.10
27.18	316.26	939.00	3.31	126.20
29.13	316.54	938.80	5.72	81.10
30.10	315.95	938.70	1.99	84.00

Table A-7. Upwind data of ZAGL, potential temperature, pressure, wind speed, and wind direction for run 4, 13 June, 1987, 1620 MST.

ZAGL (m)	θ °K	P mb	Wind Speed m/s	Wind Direction °
.00	321.97	945.40	4.37	79.70
.49	321.42	945.30	2.67	243.50
2.46	320.46	945.10	2.34	260.70
4.42	319.98	944.90	2.87	255.80
7.35	319.10	944.60	2.61	252.10
9.31	319.61	944.40	2.54	267.20
11.27	319.18	944.20	2.54	272.20
13.22	318.98	944.00	1.58	223.50
14.20	318.83	943.90	2.72	181.70
16.15	318.36	943.70	1.69	221.20
18.10	318.72	943.50	1.51	232.10
19.08	318.81	943.40	2.96	282.60
21.04	319.23	943.20	1.15	267.40
22.99	318.97	943.00	3.17	245.10
24.95	318.97	942.80	2.78	293.40
25.93	318.73	942.70	1.53	224.10
26.91	318.86	942.60	1.77	224.50
27.88	318.75	942.50	2.74	258.30
28.86	318.91	942.40	1.63	309.70

Table A-8. Downwind data of ZAGL, potential temperature, pressure, wind speed, and wind direction for run 4, 13 June, 1987, 1620 MST.

ZAGL (m)	θ °K	P mb	Wind Speed m/s	Wind Direction °
.00	314.77	944.20	1.79	232.30
.49	315.92	944.10	2.15	239.40
2.43	317.38	943.90	1.80	261.60
4.38	317.87	943.70	1.91	256.00
7.30	318.02	943.40	1.76	292.10
8.28	318.34	943.30	1.84	272.40
10.23	318.41	943.10	1.50	271.30
11.21	318.40	943.00	1.53	260.70
14.14	318.42	942.70	1.53	265.70
18.04	318.45	942.30	1.41	267.10
19.02	318.56	942.20	.00	.00
20.00	318.83	942.10	1.59	21.70
20.98	318.66	942.00	.00	.00
22.93	318.76	941.80	1.89	7.30
25.87	318.78	941.50	2.00	10.40
28.81	318.78	941.20	.71	253.90
30.76	318.81	941.00	1.02	337.80

Table A-9. Upwind data of ZAGL, potential temperature, pressure, wind speed, and wind direction for run 5, 14 June, 1987, 1540 MST.

ZAGL (m)	θ °K	P mb	Wind Speed m/s	Wind Direction °
.00	320.40	941.80	5.83	231.30
1.96	319.73	941.40	4.64	239.20
4.91	319.05	941.10	3.89	213.70
5.89	319.32	941.00	3.43	.00
7.84	318.81	940.80	3.19	188.30
8.82	319.41	940.70	3.92	249.50
9.81	319.14	940.60	3.27	247.00
10.79	319.46	940.50	3.18	239.80
11.77	318.80	940.40	2.64	232.60
12.75	319.52	940.30	4.22	244.30
15.69	318.88	940.00	2.48	236.10
16.67	318.91	939.90	1.70	156.80
18.63	318.92	939.70	5.06	260.20
20.59	318.74	939.50	1.96	280.60
21.57	318.71	939.40	5.23	241.40
22.55	318.85	939.30	1.24	325.50
23.53	318.80	939.20	.92	117.70
26.47	318.73	938.90	5.59	239.00
28.43	318.77	938.70	1.94	266.70
29.41	318.81	938.60	5.03	230.70

Table A-10. Downwind data of ZAGL, potential temperature, pressure, wind speed, and wind direction for run 5, 14 June, 1987, 1540 MST.

ZAGL (m)	θ °K	P mb	Wind Speed m/s	Wind Direction °
.00	315.63	940.60	1.40	219.50
.49	315.69	940.50	3.67	292.90
1.46	316.28	940.40	3.35	231.60
2.44	317.44	940.30	2.38	237.70
3.41	317.69	940.20	1.83	236.50
4.39	317.99	940.10	3.61	210.60
5.37	318.62	940.00	3.36	210.40
6.35	318.65	939.90	3.98	226.80
7.33	318.69	939.80	4.36	216.50
8.31	318.72	939.70	4.54	222.00
9.29	318.76	939.60	3.33	227.40
11.25	318.76	939.40	4.26	223.20
13.21	318.78	939.20	4.12	220.30
15.17	318.83	939.00	4.10	240.20
16.15	318.95	938.90	5.28	228.00
19.10	319.02	938.60	4.84	238.10
20.08	319.32	938.50	4.11	231.50
24.01	319.24	938.10	2.76	232.80
27.94	319.24	937.70	3.89	246.00
30.89	319.05	937.40	3.52	239.60

Table A-11. Upwind data of ZAGL, specific humidity, pressure, wind speed, and wind direction for run 1, 10 June, 1987, 1330 MST.

ZAGL (m)	q Kg/Kg	P mb	Wind Speed m/s	Wind Direction °
.00	.0057	946.90	4.10	105.00
2.90	.0055	946.30	2.52	100.30
7.73	.0056	945.80	3.70	87.60
8.69	.0056	945.70	3.15	92.70
10.62	.0054	945.50	3.18	83.30
13.51	.0059	945.20	6.48	101.00
14.48	.0059	945.10	6.58	97.10
15.44	.0057	945.00	5.61	97.20
16.41	.0057	944.90	1.70	169.00
17.38	.0056	944.80	1.90	183.00
18.34	.0054	944.70	1.80	162.00
22.21	.0054	944.30	4.20	127.90
25.10	.0054	944.00	1.40	165.00
26.07	.0054	943.90	2.40	192.00
28.00	.0055	943.70	2.00	180.00
28.96	.0055	943.60	4.41	126.30

Table A-12. Downwind data of ZAGL, specific humidity, pressure, wind speed, and wind direction for run 1, 10 June, 1987, 1330 MST.

ZAGL (m)	q Kg/Kg	P mb	Wind Speed m/s	Wind Direction °
.00	.0088	944.00	3.70	153.00
2.41	.0068	943.70	2.20	152.00
3.38	.0061	943.60	2.20	138.00
4.35	.0064	943.50	1.60	.00
5.31	.0058	943.40	2.20	178.00
6.28	.0057	943.30	5.10	147.00
12.08	.0059	942.70	5.40	139.00
13.05	.0066	942.60	8.10	117.00
14.02	.0060	942.50	3.40	151.00
14.99	.0058	942.40	2.70	166.00
15.96	.0057	942.30	5.90	194.00
16.93	.0059	942.20	5.90	194.00
18.87	.0058	942.00	3.60	161.00
19.83	.0058	941.90	6.60	157.00
21.77	.0058	941.70	5.20	161.00
22.74	.0063	941.60	3.20	158.00
23.71	.0067	941.50	4.30	75.00
24.68	.0058	941.40	6.90	144.00
25.65	.0066	941.30	4.30	181.00
26.62	.0065	941.20	4.90	116.00
28.56	.0061	941.00	4.60	134.00
29.53	.0059	940.90	5.90	154.00

Table A-13. Upwind data of ZAGL, specific humidity, pressure, wind speed, and wind direction for run 2, 10 June, 1987, 1530 MST.

ZAGL (m)	q Kg/Kg	P mb	Wind Speed m/s	Wind Direction °
.00	.0062	940.10	2.58	.20
.98	.0062	940.00	5.21	319.10
1.96	.0062	939.90	2.29	349.00
4.90	.0061	939.60	3.73	.00
5.88	.0061	939.50	4.12	20.00
7.84	.0060	939.30	3.45	14.80
10.77	.0060	939.00	4.30	38.80
11.75	.0059	938.90	4.83	338.30
13.70	.0061	938.70	3.44	.00
14.68	.0061	938.60	4.01	281.90
17.61	.0060	938.30	2.26	6.00
18.58	.0060	938.20	3.47	6.40
21.51	.0061	937.90	2.86	336.00
22.49	.0060	937.80	2.42	24.10
23.46	.0061	937.70	3.60	343.80
25.42	.0060	937.50	3.83	15.10
26.39	.0060	937.40	3.33	336.40
29.32	.0060	937.10	3.11	342.50

Table A-14. Downwind data of ZAGL, specific humidity, pressure, wind speed, and wind direction for run 2, 10 June, 1987, 1530 MST.

ZAGL (m)	q Kg/Kg	P mb	Wind Speed m/s	Wind Direction °
.00	.0086	940.40	3.18	69.80
.97	.0082	940.30	6.00	20.90
1.94	.0083	940.20	5.45	11.50
2.92	.0073	940.10	1.56	11.50
5.84	.0067	939.80	6.66	23.40
8.76	.0065	939.50	5.64	26.40
9.74	.0064	939.40	8.08	37.90
10.71	.0060	939.30	6.90	335.70
12.67	.0060	939.10	5.15	18.40
13.64	.0058	939.00	4.60	26.80
14.61	.0057	938.90	5.15	345.30
16.56	.0056	938.70	4.52	6.80
17.54	.0056	938.60	5.32	348.50
18.52	.0055	938.50	4.53	.20
19.49	.0056	938.40	4.72	.00
21.44	.0056	938.20	4.92	44.00
23.39	.0055	938.00	5.10	8.70
25.35	.0057	937.80	5.98	28.10
27.30	.0056	937.60	4.86	17.10
31.20	.0056	937.20	5.24	17.40

Table A-15. Upwind data of ZAGL, specific humidity, pressure, wind speed, and wind direction for run 3, 11 June, 1987, 1620 MST.

ZAGL (m)	q Kg/Kg	P mb	Wind Speed m/s	Wind Direction °
.00	.0056	944.00	4.20	99.60
1.46	.0056	943.70	4.12	142.20
4.38	.0057	943.40	5.76	143.00
6.33	.0057	943.20	5.41	135.20
8.27	.0058	943.00	4.42	144.00
13.12	.0057	942.50	4.57	142.90
15.06	.0057	942.30	2.81	134.10
17.97	.0056	942.00	3.18	146.60
20.89	.0056	941.70	2.14	142.10
22.83	.0056	941.50	2.49	157.20
27.69	.0056	941.00	4.69	148.10

Table A-16. Downwind data of ZAGL, specific humidity, pressure, wind speed, and wind direction for run 3, 11 June, 1987, 1620 MST.

ZAGL (m)	q Kg/Kg	P mb	Wind Speed m/s	Wind Direction °
.00	.0112	941.70	1.28	141.80
3.87	.0091	941.40	2.33	131.60
4.84	.0070	941.30	2.37	128.60
6.78	.0064	941.10	3.08	96.90
7.75	.0062	941.00	2.67	107.20
8.72	.0063	940.90	2.16	137.40
9.69	.0058	940.80	1.73	79.80
10.66	.0060	940.70	3.79	94.00
11.63	.0057	940.60	1.95	93.30
12.60	.0059	940.50	3.62	99.60
13.57	.0057	940.40	1.51	116.40
14.55	.0057	940.30	1.95	129.10
15.52	.0057	940.20	2.21	119.30
16.49	.0060	940.10	3.37	96.90
17.46	.0058	940.00	2.24	127.70
18.43	.0060	939.90	3.27	97.90
19.40	.0059	939.80	4.12	91.90
20.38	.0057	939.70	2.64	117.40
23.29	.0059	939.40	3.48	96.80
24.27	.0056	939.30	1.90	122.80
25.24	.0056	939.20	2.59	134.70
26.21	.0057	939.10	.98	109.10
27.18	.0056	939.00	3.31	126.20
29.13	.0059	938.80	5.72	81.10
30.10	.0057	938.70	1.99	84.00

Table A-17. Upwind data of ZAGL, specific humidity, pressure, wind speed, and wind direction for run 4, 13 June, 1987, 1620 MST.

ZAGL (m)	q Kg/Kg	P mb	Wind Speed m/s	Wind Direction °
.00	.0062	945.40	4.37	79.70
2.46	.0063	945.10	2.34	260.70
4.42	.0063	944.90	2.87	255.80
7.35	.0062	944.60	2.61	252.10
9.31	.0059	944.40	2.54	267.20
11.27	.0060	944.20	2.54	272.20
13.22	.0059	944.00	1.58	223.50
14.20	.0060	943.90	2.72	181.70
16.15	.0062	943.70	1.69	221.20
18.10	.0062	943.50	1.51	232.10
19.08	.0059	943.40	2.96	282.60
21.04	.0060	943.20	1.15	267.40
22.99	.0059	943.00	3.17	245.10
24.95	.0060	942.80	2.78	293.40
25.93	.0061	942.70	1.53	224.10
26.91	.0061	942.60	1.77	224.50
27.88	.0060	942.50	2.74	258.30
28.86	.0061	942.40	1.63	309.70

Table A-18. Downwind data of ZAGL, specific humidity, pressure, wind speed, and wind direction for run 4, 13 June, 1987, 1620 MST.

ZAGL (m)	q Kg/Kg	P mb	Wind Speed m/s	Wind Direction °
.00	.0122	944.20	1.79	232.30
.49	.0108	944.10	2.15	239.40
2.43	.0081	943.90	1.80	261.60
4.38	.0072	943.70	1.91	256.00
7.30	.0069	943.40	1.76	292.10
8.28	.0066	943.30	1.84	272.40
10.23	.0062	943.10	1.50	271.30
11.21	.0062	943.00	1.53	260.70
14.14	.0061	942.70	1.53	265.70
18.04	.0061	942.30	1.41	267.10
19.02	.0063	942.20	.00	.00
20.00	.0061	942.10	1.59	21.70
20.98	.0063	942.00	.00	.00
22.93	.0061	941.80	1.89	7.30
25.87	.0060	941.50	2.00	10.40
28.81	.0062	941.20	.71	253.90

Table A-19. Upwind data of ZAGL, specific humidity, pressure, wind speed, and wind direction for run 5, 14 June, 1987, 1540 MST.

ZAGL (m)	q Kg/Kg	P mb	Wind Speed m/s	Wind Direction °
.00	.0066	941.80	5.83	231.30
1.96	.0063	941.40	4.64	239.20
4.91	.0060	941.10	3.89	213.70
5.89	.0059	941.00	3.43	.00
7.84	.0059	940.80	3.19	188.30
8.82	.0060	940.70	3.92	249.50
9.81	.0058	940.60	3.27	247.00
10.79	.0059	940.50	3.18	239.80
11.77	.0059	940.40	2.64	232.60
12.75	.0058	940.30	4.22	244.30
15.69	.0059	940.00	2.48	236.10
16.67	.0059	939.90	1.70	156.80
18.63	.0060	939.70	5.06	260.20
20.59	.0060	939.50	1.96	280.60
21.57	.0061	939.40	5.23	241.40
22.55	.0060	939.30	1.24	325.50
23.53	.0059	939.20	.92	117.70
26.47	.0060	938.90	5.59	239.00
28.43	.0059	938.70	1.94	266.70
29.41	.0061	938.60	5.03	230.70

Table A-20. Downwind data of ZAGL, specific humidity, pressure, wind speed, and wind direction for run 5, 14 June, 1987, 1540 MST.

ZAGL (m)	q Kg/Kg	P mb	Wind Speed m/s	Wind Direction °
.00	.0117	940.50	3.67	292.90
1.46	.0112	940.40	3.35	231.60
2.44	.0106	940.30	2.38	237.70
3.41	.0098	940.20	1.83	236.50
4.39	.0072	940.10	3.61	210.60
5.37	.0064	940.00	3.36	210.40
6.35	.0065	939.90	3.98	226.80
7.33	.0063	939.80	4.36	216.50
8.31	.0063	939.70	4.54	222.00
9.29	.0061	939.60	3.33	227.40
11.25	.0061	939.40	4.26	223.20
13.21	.0062	939.20	4.12	220.30
15.17	.0060	939.00	4.10	240.20
16.15	.0060	938.90	5.28	228.00
19.10	.0059	938.60	4.84	238.10
20.08	.0062	938.50	4.11	231.50
24.01	.0061	938.10	2.76	232.80
27.94	.0063	937.70	3.89	246.00